Evolutionary Systematics. 9 2025, 7–31 | DOI 10.3897/evolsyst.9.135431

PENSOFT

EVOLUTIONARY SYSTEMATICS

Systematics of the *Dendropsophus leucophyllatus* species group (Anura, Hylidae) from the Chocó region of Ecuador, with description of a new species

P. Doménica Aguirre[1,2], Katherine Apunte[1], Santiago R. Ron[1]

1 *Museo de Zoología, Escuela de Biología, Pontificia Universidad Católica del Ecuador, Av. 12 de Octubre y Roca, Aptdo. 17-01-2184, Quito, Ecuador*

2 *Department of Biological Science, Florida State University, Tallahassee, FL 32306, USA*

https://zoobank.org/044BF460-92DB-4715-A639-DF2CF34AA07C

Corresponding author: Santiago R. Ron (santiago.r.ron@gmail.com)

Academic editor: Alexander Haas ♦ **Received** 27 August 2024 ♦ **Accepted** 8 January 2025 ♦ **Published** 21 February 2025

Abstract

The *Dendropsophus leucophyllatus* group is composed by 19 species distributed from Central America to the Atlantic Forest of Brazil. Only one species is known from the Chocó region, *D. ebraccatus*, which is also distributed in Central America. Previous studies suggested the existence of two species masked under "*D. ebraccatus*". The only other species of *Dendropsophus* in the Chocó lowlands of Ecuador is *D. gryllatus*, an elusive species never included in phylogenetic analyses. In the present study, we review the systematics of both species based on morphological, genetic, and bioacoustic data. For phylogenetic analyses, we sequenced four mitochondrial genes (12S, 16S, COI, ND1, including flanking tRNAs) and two nuclear genes (TYR, POMC). Our results indicate that the populations of "*D. ebraccatus*" from the Chocó of Ecuador represent a new species, not most closely related to *D. ebraccatus* from Central America, but to *D. gryllatus*. The new species inhabits tropical rainforest and piedmont evergreen forest of NW Ecuador and SW Colombia. Populations of the new species differ from *D. gryllatus* by having larger body size and by the presence of an hourglass-shaped dorsal mark. The new species differs from *D. ebraccatus* from Central America by the absence of a clear band under the eye, by having well defined dorsal spots and by having a distinct advertisement call. Both species appear to be allopatric and, according to our time-tree, diverged from each other during the late Pliocene.

Key Words

Advertisement calls, Chocó rainforest, Colombia, *Dendropsophus cannatellai* sp. nov., *Dendropsophus gryllatus*, phylogeny

Introduction

The Neotropical region exhibits a remarkable species richness, partly as a result of its favorable climatic and geographical conditions, which foster the diversification of various groups, particularly amphibians. The genus *Dendropsophus*, belonging to the Hylidae family, comprises 107 documented species (Frost 2024) that are categorized into nine taxonomic groups by Orrico et al. (2021): *Dendropsophus ruschii*, *D. decipiens*, *D. parviceps*, *D. molitor*, *D. columbianus*, *D. marmoratus*, *D. minutus*, *D. leucophyllatus*, and *D. microcephalus*.

The *Dendropsophus leucophyllatus* group comprises 19 species with the following synapomorphic diagnostic characters: (1) expanded cartilaginous plate in the nasal cartilages, and (2) males with pectoral glands arranged in two clear distinct patches (Orrico et al. 2021). It originated in the early Miocene from ancestors distributed in the Pacific Dominion region (Pirani et al. 2020). The group has been the focus of numerous taxonomic revisions (Duellman 1974; Chek et al. 2001; Rivera-Correa and Orrico 2013; Caminer et al. 2017; Orrico et al. 2021). One of the most comprehensive reviews of the group was carried out by Caminer et al. (2017). At the time,

Copyright *P. Doménica Aguirre et al.* This is an open access article distributed under the terms of the Creative Commons Attribution License (CC BY 4.0), which permits unrestricted use, distribution, and reproduction in any medium, provided the original author and source are credited.

the group was composed by 10 species. Using genetic, morphological and bioacustic data, Caminer et al. (2017) found nine candidate species within the Amazonian species "*D. leucophyllatus*" and "*D. triangulum*". They described two of those species and highlighted the existence of cryptic diversity and unresolved alpha-taxonomic issues in the group. More recently, Orrico et al. (2021) showed its phylogenetic position within *Dendropsophus*, reexamined the species content of the group, provided a summary of its distribution, and discussed its morphological synapomorphies. They also discussed the possibility that *D. gryllatus*, a species of unknown relationships, is a member of the *D. leucophyllatus* group (see below).

One of the species of the group with a large distribution is *D. ebraccatus* (Cope, 1874), the hourglass treefrog, from Central America and the Chocó region in NW South America (Pirani et al. 2021). It is a small, brightly colored species with a distinctive hourglass pattern on its dorsum. It has a distinctive call, with high-pitched trilling notes (Duellman 1970). Pirani et al. (2020) conducted a study using genome-wide SNP data to investigate the diversity, phylogeny, and biogeography of the *Dendropsophus leucophyllatus* species group. One of their phylogenies recovered *D. ebraccatus* as paraphyletic, suggesting the existence of an undescribed species. Another phylogeny recovered a monophyletic *D. ebraccatus* but with a deep divergence between Central American and Chocoan populations of Ecuador (~12 million years), also suggesting the existence of more than one species within "*D. ebraccatus*". Therefore, the available evidence (i.e., weak support for "*D. ebraccatus*" monophyly and genomic evidence of a divergence time between populations > 10 My), strongly indicates the existence of at least two species within "*D. ebraccatus*", one in Central America and the other in the Chocó region of Ecuador.

The only other member of *Dendropsophus* in the Chocó region is *D. gryllatus* (Duellman, 1973), the Pacific Lowland Tree frog. It is endemic to western Ecuador and is characterized by small size and tan or brown coloration with dark margins on the limbs. Its name refers to its cricket-like call (Duellman 1973). The evolutionary affinities of *D. gryllatus* are unknown. Duellman (1973) assigned it to the "*Hyla microcephala*" species group and Faivovich et al. (2005) maintained that assignment (*Dendropsophus microcephalus* group). Orrico et al. (2021) noted that the species description mentions the presence of a long cloacal sheath, a feature of the *D. minutus* group. Despite this, the species' coloration and advertisement call resemble those of the *D. leucophyllatus* group (Orrico et al. 2021). Still, there was insufficient evidence to assign the species to either group. After its description, *D. gryllatus* has been intermittently documented and is rare in scientific collections, being recorded only from few localities (Duellman 1973; Michelsohn et al. 2022; Ron et al. 2024). Its conservation status is Critically Endangered with declining populations (Ortega-Andrade et al. 2021).

The aim of this study is to test the existence of two species masked under *Dendropsophus ebraccatus* and, if needed, describe the new species. The second aim was to determine the phylogenetic position of *D. gryllatus*. Our review is based on the morphological characterization of specimens, supplemented with phylogenetic analyses and bioacoustic information.

Materials and methods

Ethics statement

Following ethical and technical guidelines, voucher specimens and tissue samples were collected in accordance with licenses N° MAAE-DBI-CM-2022-0230 and N° MAAE-CMARG-2022-0488-01045, granted to Pontificia Universidad Católica de Ecuador by the Ministerio de Ambiente del Ecuador.

Species concept

We follow the evolutionary species concept which considers a species as a "a single lineage of ancestor-descendant populations of organisms which maintains its identity from other such lineages, and which has its own evolutionary tendencies and historical fate" (Wiley 1978). Identity with respect to other lineages was assessed by examining genetic, bioacoustic, and morphological characters in an integrative framework.

Phylogenetic analyses

Phylogenetic analyses were performed on DNA sequences extracted from tissues deposited at the biobank of the Museum of Zoology (QCAZ) at Pontificia Universidad Católica del Ecuador. We sequenced at least one adult individual from each available population for a total of seven individuals of *D. ebraccatus*. Only one population was available for *D. gryllatus* from which we sequenced three individuals, representative of the range of morphological variation within the population. For the phylogenetic analyses, we sequenced DNA of the mitochondrial genes 12S ribosomal RNA, tRNA-Val, 16S ribosomal RNA, tRNA-Leu, cytochrome oxidase c subunit I (COI), NADH dehydrogenase subunit 1 (ND1), tRNA-Ile, tRNA-Gln, and the nuclear genes proopiomelanocortin A (POMC) and tyrosinase (TYR). DNA was extracted from 95% ethanol-preserved tissues (liver or muscle). PCR amplification was carried under standard conditions. The primers used for the 12S gene amplification were MVZ59, MVZ50/16S-frog, and WL384, while for the 16S gene amplification, the primers used were 16L19 and 16H36E. For the COI gene amplification, we used the primers LCO1490 and HCO2198, whereas the ND1 gene amplification was carried out using WL379 and tMet-frog primers. The POMC gene amplification utilized POMC-1, POMC-2/tPhe2-frog, and tRNA-Val-Pauly primers and for the TYR gene amplification, we used Tyr1C and Tyr1G primers. Sanger sequencing of PCR products was performed by Macrogen Inc., Seoul, Korea.

Additionally, we obtained homologous sequences from Orrico et al. (2021) available at GenBank. We also included sequences of cytochrome b (CytB), and the nuclear genes rhodopsin (RHOD), recombination activation gene 1 (RAG-1), and seventh in absentia (SIAH) published by Orrico et al. (2021). For a complete list of the GenBank sequences used, see Appendix S3 in Orrico et al. (2021).

For sequence assembly, we used software GeneiousPro 9.1.8 (Kearse et al. 2012). We employed Mesquite v.3.02 (Maddison 2008) for matrix alignment, with MAFFT extension (Katoh et al. 2002), with the L-INS-I alignment algorithm and the default settings --localpair --maxiterate 1000. The final dataset comprised DNA sequences from 203 individuals (Table 1 lists vouchers and GenBank accession numbers for newly generated sequences). The concatenated final matrix had 7691 bp. Within this matrix, gene content was: 12S (996 bp), tRNA-Val (68 bp), 16S (1844 bp), tRNA-Leu (73 bp), NADH dehydrogenase subunit 1 ND1 (959 bp), tRNAIle (69 bp), tRNAGln (58 bp, partial sequence), CO1 (662 bp) and cytochrome b CytB (887 bp, partial sequence), alongside the nuclear genes RAG1 (425 bp, partial sequence), rhodopsin (314 bp), tyrosinase (533 bp), seven in absentia SIAH1 (395 bp), proopiomelanocortin POMC (473 bp). The concatenated matrix is available in Zenodo.org under https://zenodo.org/records/14191769, DOI: 10.5281/zenodo.14191769. To facilitate linking sequences with vouchers, we named each terminal in the matrix with its species followed by its voucher number (if available from the literature).

To infer phylogenetic relationships, we used maximum likelihood (ML) as optimality criterion with IQ-TREE multicore version 2.2.0.7 under default settings (Nguyen et al. 2015). The concatenated matrix was partitioned based on gene and codon position (Chernomor et al. 2016) and analyzed under model GTR + R + I. To evaluate branch support, we conducted 1000 ultrafast bootstrap (BS) (Hoang et al. 2018) searches and 1000 replicates for the SH-like approximate likelihood ratio test (SH-aLRT). Branches were considered to have robust support if their ultrafast bootstrap values were higher than 94% and SH-aLRT values were higher than 79%. The terminal used to root the tree was *Pseudis minuta*.

Using the best maximum likelihood tree, we estimated a time-tree with the least square dating method (To et al. 2016) in IQ-TREE. We used one calibration point based on the phylogeny by Hime et al. (2021): 37.8 My for the divergence between *Pseudis minuta* and *Dendropsophus sarayacuensis*.

Phylogenies based on mitochondrial genes can be inconsistent with the evolutionary history of the species as result of its uniparental inheritance, introgression, and incomplete lineage sorting. Therefore, taxonomic decisions based exclusively on mitochondrial DNA can be problematic (Hillis 2019). To provide independent genetic evidence of the genetic distinctiveness of the new species relative to its sister species, we generated a phylogenetic network for the gene tyrosinase. The network was built with SplitsTree v. 4.19.2 (Huson and Bryant 2006) using the NeighborNet method under HKY85 distances. We note that the genomic distinctiveness (independent of mitochondrial DNA evidence) between the new species and *D. ebraccatus* was already provided by Pirani et al. (2021).

To calculate genetic distances, we used the online program DIVEIN (Deng et al. 2010) with sequences of the 16S rRNA gene.

Morphological comparisons and descriptions

We recorded external morphological characters, such as the size and shape of the head, limbs, and body, as well as coloration patterns. Our comparisons focused on *Dendropsophus ebraccatus* from Central America and Ecuador, and *D. gryllatus* (Pirani et al. 2020; Orrico et al. 2021). We analyzed 135 specimens of *D. ebraccatus* available at the Museo de Zoología (acronym QCAZ) at Pontificia Universidad Católica del Ecuador, from Mexico, Panama, and Ecuador. For *Dendropsophus gryllatus*, we analyzed 10 individuals from two localities in Ecuador. Detailed information for examined specimens is provided in Suppl. material 1, table S1. The specimens were preserved in 10% formalin and stored in 70% ethanol. We compared quantitative and qualitative morphological characters following definitions and terminology by Duellman (1970). The term "distinct" was used to describe an individual with clearly distinguishable features, whereas the term "indistinct" was used to describe hardly perceptible features. Sex and reproductive status were determined by inspecting secondary sexual characters such as vocal sacs, vocal slits, and nuptial pads, or by direct gonadal examination. Maturity in males was determined by testicle size; in females, big ovarian eggs or convoluted oviducts were considered indicative of adulthood (Duellman and Lehr 2009).

Table 1. GenBank accession numbers for newly generated DNA sequences used in the phylogenetic analyses.

Voucher	Species	12S	16S	CO1	ND1	POMC	TYR
QCAZ 15519	*D. cannatellai* sp. nov.	PP295263	PP475413	PP301802	NA	PP301805	PP301809
QCAZ 27207	*D. cannatellai* sp. nov.	NA	PP475414	NA	NA	PP301806	PP301810
QCAZ 40847	*D. cannatellai* sp. nov.	PP295264	PP481929	PP301801	PP301804	NA	NA
QCAZ 55530	*D. cannatellai* sp. nov.	PP295265	PP317604	NA	NA	PP301807	PP301811
QCAZ 66631	*D. cannatellai* sp. nov.	PP295266	PP475415	NA	NA	PP301808	PP301812
QCAZ 78257	*D. cannatellai* sp. nov.	PP295267	PP317603	NA	NA	NA	NA
QCAZ 75534	*D. gryllatus*	PP455270	PP317601	NA	PP301803	NA	PV029256
QCAZ 75535	*D. gryllatus*	NA	PV067161	NA	NA	NA	PV029257
QCAZ 75540	*D. gryllatus*	PP295268	PP317602	NA	NA	NA	PP301813

We only give color information in the "Definition" and "Diagnosis" sections to shorten the description of the new species and prevent the subjectivity in verbal descriptions of coloration (Vences 2020). To document more effectively color variation, we present high-resolution images of the holotype and several paratypes (life and preservative) of the new species and several specimens of *D. gryllatus*.

The SVL (snout-vent length) was measured in 129 paratypes. In the holotype we took the following measurements (measurement methodology in parenthesis, otherwise measurements were made as described in Duellman 1970): foot length; tibia length; femur length (distance from knee to vent); arm length (distance from arm base to elbow); head length; head width; eye diameter (distance between the anterior and posterior borders of the visible eye); tympanum diameter (horizontal distance between the peripheral borders of the tympanic annulus); interorbital distance (distance between the medial edge of the orbits); internarial distance (distance between the inner edges of the nostrils); eye-snout distance (distance from the orbit to the tip of the snout). All measurements were made using a digital caliper with a 0.01 mm precision.

A pair of *D. cannatellai* sp. nov. from Río Silanche, laid a clutch of eggs in captivity and the tadpoles were raised for one year. We present photos of the tadpole, juvenile and subadult individuals in Figs 10, 11.

Bioacoustic analyses

We recorded in-situ calls of *D. cannatellai* sp. nov. using Olympus OM System LS-10 and LS-14 recorders along with a Sennheiser Professional MKE600 Shotgun Microphone. Additionally, we used recordings from the Macaulay Library of five individuals of *Dendropsophus gryllatus* from Los Ríos, Río Palenque (catalog numbers: ML 194007, 194008, 194009 and 194010). Additionally, we included an aggressive call from one individual (ML 194006), shown in Fig. 5. For *Dendropsophus ebraccatus* we analyzed recordings from five individuals from Mexico, Guatemala, and Panama, with catalog number ML 193729 (Fig. 4), ML 193729, ML 210735, ML 210751, and ML 237602 (Suppl. material 4, figure S3). Detailed voucher and locality information is provided in Suppl. material 1, table S1.

Calls were analyzed using Raven Pro 1.3 software (Cornell Lab of Ornithology 2003–2008), with a frequency resolution of 10.8 Hz. Terminology for the analysis followed a call-centered approach as outlined by Köhler et al. (2017). We measured the following variables: (1) primary note duration, (2) first secondary click duration, (3) primary note pulse duration, (4) dominant frequency of the call, (5) dominant frequency of the primary note, (6) dominant frequency of the first secondary click, and (7) inter-note interval, all defined according to Köhler et al. (2017) and explained in Table 2.

We measured these call variables for both *D. cannatellai* sp. nov. and *D. gryllatus* in advertisement and aggressive calls. We determined the call types based on the context on which they were produced and the descriptions provided by Wells and Schwartz (1984a) for *D. ebraccatus*: "advertisement calls consist of a buzz-like introductory note which may be followed by one or more secondary click notes" (p. 405). Wells and Schwartz (1984b) further describe aggressive calls, stating that they "are similar to advertisement calls, but have much higher pulse repetition rates and often are much longer" (p. 129). To assess acoustic differentiation between the newly described species (*D. cannatellai* sp. nov.) and *D. gryllatus*, we performed a Principal Component Analysis using the average values of each acoustic variable per male. All multivariate analyses were carried out using R Studio version 1.1.463 (R Core Team 2023), with visualization through ggplot2 (Wickham and Chang 2016). Only principal components with eigenvalues greater than 1 were retained for further analysis. We defined the primary note as the introductory note of a vocalization, and the secondary clicks as the short, subsequent notes or repetitions (Wells and Schwartz 1984a; Köhler et al. 2017).

Ecological niche modeling and environmental envelope

We made a Principal Component Analysis of 19 bioclimatic variables, downloaded from CHELSA (https://chelsa-climate.org), to compare the environmental envelope of occurrence localities between the new species and its sister species, *Dendropsophus gryllatus*. We considered that divergence in the environmental conditions where each species occurs would be suggestive of species-level differentiation.

We gathered documented occurrence localities for both species, as shown in Fig. 6. To avoid pseudo replication from spatial autocorrelation, we excluded localities at distances < 5 km from other localities, irrespective of species identification. At the end, we had 12 localities for the new species and 3 for *D. gryllatus*. We used the point sampling tool plugin in QGIS 3.34 (QGIS.org 2023) to extract values for 19 bioclimatic raster maps from CHELSA (Karger et al. 2021). Bioclimatic variables (listed in Suppl. material 6) are derived from precipitation and temperature data and are considered to influence the distribution of organisms. These values were used to run a Principal Components Analysis (PCA) as implemented by the *prcomp* function in R (R Core Team 2023).

Ecological niche modeling was carried out using the Wallace 2 package (Kass et al. 2023), and the models were constructed by integrating the Maximum Entropy (MaxEnt) 3.4.4 version algorithm. For the occurrence data, we used localities of *D. cannatellai* sp. nov. from museum specimens (Suppl. material 1, table S1) and from two Colombian localities in iNaturalist (observations 147931034 and 36196673). The environmental layers consisted of 19 bioclimatic layers with a resolution of 30 arcsec from WorldClim 2 (Fick and Hijmans 2017).

Table 2. Call parameters analyzed for the species' recordings.

Character	Definition
Duration of the primary note	Duration of the introductory note in the call.
Duration of the first secondary click	Duration of the second note (secondary click) in the call.
Pulse duration of the primary note	Time interval measured from one amplitude minimum to the subsequent amplitude minimum.
Dominant frequency of the call	The base/lowest frequency component of the whole call produced by the vocal cords.
Dominant frequency of the primary note	The base/lowest frequency component of the introductory note in the call.
Dominant frequency of the first secondary click	The base/lowest frequency component of the second note (secondary click) in the call.
Inter-note interval	Duration of the silent interval between consecutive notes within the call.
Number of pulses of the primary note	Number of pulses in the primary note in a call.
Pulse repetition rate of the primary note	Number of pulses per second during the primary note

In the environmental data processing module, we delimited the background extent for the study area using the minimum convex polygon function. To avoid the effects of spatial autocorrelation, we divided the occurrence data for model evaluation based on the spatial partition method using the "checkerboard 2" method, which adds another level of hierarchy to the spatial grouping, resulting in k = 4 groups with a user-specified "aggregation factor" of 2.

All model entity classes were selected: L, LQ, and H (Linear, Quadratic, and Hinge), and their possible interactions: LQH and LQHP (P = Product). Regularization multipliers were adjusted between 1 and 2. The multiplier value, categorical variable, clamping, and parallel parameters were set to default values.

For evaluating the model that best fit the data distribution, two parameters were considered: the area under the curve (AUC) and the omission rate (OR). Both values range from 0 to 1. AUC values closer to 1 and OR values closer to 0 are indicative of better model performance (Swets 1988). The final model was constructed using the MaxEnt algorithm (Phillips and Dudik 2008); species occurrences and environmental variables were configured only with the LQH parameters and the regularization multiplier set to 2, which was the best model previously obtained. Output from MaxEnt is a raster representing species probability of presence with values ranging from 0 to 1 (cloglog output format). Based on the threshold of the minimum training presence, we transformed that raster into a binary presence-absence species distribution model.

Results

Phylogeny and genetic variation

Our phylogeny has a topology similar to that of Orrico et al. (2021), except that in our analysis, *D. schubarti* is placed as sister species of the *D. microcephalus* group (Suppl. material 2, figure S1). Excluding *D. schubarti*, the *D. leucophyllatus* group is monophyletic but with weak support. Within the *D. leucophyllatus* group, there is a basal divergence between the *D. haraldschultzi* clade and the *D. leucophyllatus* clade (sensu Orrico et al. 2021; Fig. 1). Due to the position of *D. anceps*, a species from the Atlantic Forest of Brazil, the *D. leucophyllatus* clade has weak support. The remaining species form a strongly supported clade with a basal divergence between *D. elegans* + *D. salli* + *D. vraemi* and the remaining species (Fig. 1).

The phylogeny shows a paraphyletic *D. ebraccatus* with strong support. Populations of *D. ebraccatus* from Ecuador are most closely related to *D. gryllatus* (branch support 100/100 SH-aLRT/BS) than to Central American populations. These and previous results based on genomic data (Pirani et al. 2020) indicate that the populations of "*D. ebraccatus*" from the Chocó region of Ecuador represent a new species that we describe here as *D. cannatellai* sp. nov. (see details in the species description section). The clade *D. gryllatus* + *D. cannatellai* sp. nov. + *D. ebraccatus*, has weak support (37.1/88).

The uncorrected p-genetic distances for gene 16S between *D. cannatellai* sp. nov. and *D. gryllatus* are 2.9%. Distances between *D. cannatellai* sp. nov and *D. ebraccatus* range from 6.6 to 8.7%. Distances among populations of *D. ebraccatus* from Costa Rica, Nicaragua, and Belize vs. Panama and Colombia range between 0.9 and 1.9%. Distances between populations of *D. cannatellai* sp. nov. range from 0.14 to 0.42%. Intrapopulation genetic distances in the new species were 0%. See Suppl. material 8, table S4, for the p-genetic distances values.

Our phylogenetic network for the nuclear gene tyrosinase is consistent with the phylogeny in showing reciprocal monophyly between *D. cannatellai* sp. nov. and *D. gryllatus* (Suppl. material 5, figure S4).

Our chronogram estimates that *D. cannatellai* sp. nov. diverged from *D. gryllatus* during the late Pliocene. Divergence between *D. ebraccatus* and the new species + *D. gryllatus* is deep, ~17 Mya. For the complete chronogram of *Dendropsophus* (see Suppl. material, figure S3).

Bioacoustic analyses

Bioacoustic data are presented in Table 3 and character loadings for Principal Components Analyses are shown in Table 4. *Dendropsophus cannatellai* sp. nov. and *D. gryllatus* exhibit acoustic differences, especially in Dominant frequency and Pulse rate (Fig. 3, Table 3).

The dominant frequency of the advertisement calls in *Dendropsophus cannatellai* sp. nov. is lower (range 3169.9–3498.7 Hz) compared to that of *D. gryllatus*

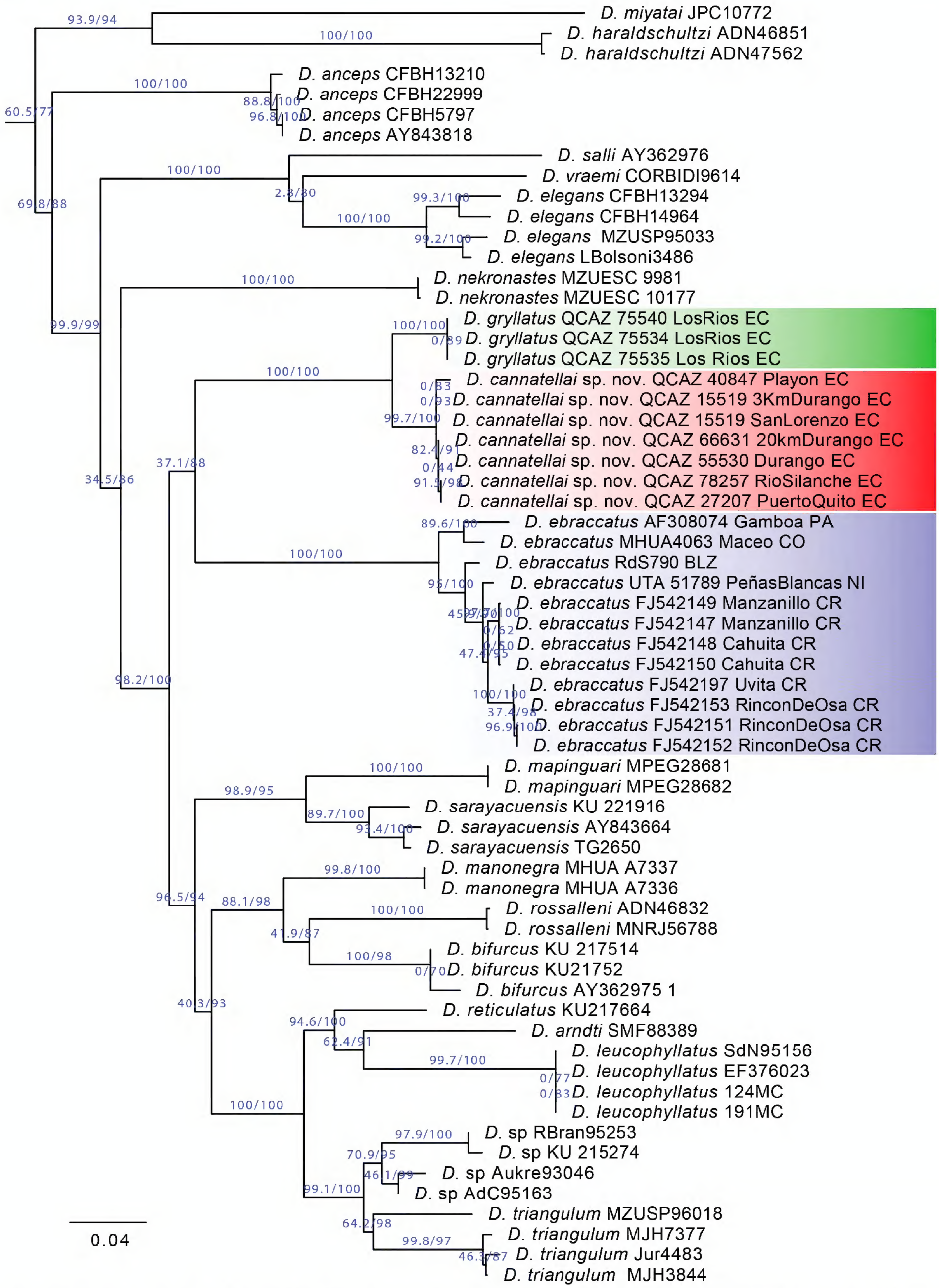
D. miyatai JPC10772
D. haraldschultzi ADN46851
D. haraldschultzi ADN47562
D. anceps CFBH13210
D. anceps CFBH22999
D. anceps CFBH5797
D. anceps AY843818
D. salli AY362976
D. vraemi CORBIDI9614
D. elegans CFBH13294
D. elegans CFBH14964
D. elegans MZUSP95033
D. elegans LBolsoni3486
D. nekronastes MZUESC 9981
D. nekronastes MZUESC 10177
D. gryllatus QCAZ 75540 LosRios EC
D. gryllatus QCAZ 75534 LosRios EC
D. gryllatus QCAZ 75535 Los Rios EC
D. cannatellai sp. nov. QCAZ 40847 Playon EC
D. cannatellai sp. nov. QCAZ 15519 3KmDurango EC
D. cannatellai sp. nov. QCAZ 15519 SanLorenzo EC
D. cannatellai sp. nov. QCAZ 66631 20kmDurango EC
D. cannatellai sp. nov. QCAZ 55530 Durango EC
D. cannatellai sp. nov. QCAZ 78257 RioSilanche EC
D. cannatellai sp. nov. QCAZ 27207 PuertoQuito EC
D. ebraccatus AF308074 Gamboa PA
D. ebraccatus MHUA4063 Maceo CO
D. ebraccatus RdS790 BLZ
D. ebraccatus UTA 51789 PeñasBlancas NI
D. ebraccatus FJ542149 Manzanillo CR
D. ebraccatus FJ542147 Manzanillo CR
D. ebraccatus FJ542148 Cahuita CR
D. ebraccatus FJ542150 Cahuita CR
D. ebraccatus FJ542197 Uvita CR
D. ebraccatus FJ542153 RinconDeOsa CR
D. ebraccatus FJ542151 RinconDeOsa CR
D. ebraccatus FJ542152 RinconDeOsa CR
D. mapinguari MPEG28681
D. mapinguari MPEG28682
D. sarayacuensis KU 221916
D. sarayacuensis AY843664
D. sarayacuensis TG2650
D. manonegra MHUA A7337
D. manonegra MHUA A7336
D. rossalleni ADN46832
D. rossalleni MNRJ56788
D. bifurcus KU 217514
D. bifurcus KU21752
D. bifurcus AY362975 1
D. reticulatus KU217664
D. arndti SMF88389
D. leucophyllatus SdN95156
D. leucophyllatus EF376023
D. leucophyllatus 124MC
D. leucophyllatus 191MC
D. sp RBran95253
D. sp KU 215274
D. sp Aukre93046
D. sp AdC95163
D. triangulum MZUSP96018
D. triangulum MJH7377
D. triangulum Jur4483
D. triangulum MJH3844
0.04

Figure 1. Maximum likelihood tree of the *Dendropsophus leucophyllatus* group based on concatenated DNA sequences of mitochondrial and nuclear genes. Blue numbers on branches show SH-aLRT values (before slash) and ultrafast bootstrap support values (after slash). Support values not shown for intraspecific relationships, except for deepest nodes within *D. ebraccatus*.

Table 3. Descriptive statistics of advertisement calls of *Dendropsophus cannatellai* sp. nov. and *D. gryllatus*. The *n* values represent the number of males analyzed. The mean and standard deviation (Mean ± SD) are provided, with the range shown in parentheses.

	***D. cannatellai* (n = 4)**	***D. gryllatus* (n = 4)**	***D. ebraccatus* (n = 5)**
Duration of the primary note (s)	0.11 ± 0.02 (0.09–0.13)	0.11 ± 0.01 (0.10–0.12)	0.21 ± 0.02 (0.19–0.23)
Duration of the first secondary click (s)	0.03 ± 0.01 (0.02–0.03)	0.03 ± 0.02 (0.02–0.03)	0.05 ± 0.01 (0.03–0.05)
Pulse duration of the primary note (s)	0.09 ± 0.01 (0.08–0.09)	0.10 ± 0.01 (0.09–0.10)	0.16 ± 0.01 (0.15–0.17)
Dominant frequency of the call (Hz)	3274.74 ± 155.74 (3169.91–3498.68)	3606.80 ± 93.44 (3531.40–3644.50)	2386.23 ± 1218.38 (559.86–2964.40)
Dominant frequency of the primary note (Hz)	3294.93 ± 142.00 (3187.50–3493.48)	3604.13 ± 77.28 (3563.70–3732.40)	2502.86 ± 980.60 (1033.59–3057.71)
Dominant frequency of the first secondary click (Hz)	3255.37 ± 188.38 (3181.65–3583.00)	3682.15 ± 106.58 (3531.40–3789.80)	2065.40 ± 1715.41 (86.13–3122.31)
Inter-note interval (s)	0.09 ± 0.01 (0.08–0.10)	0.10 ± 0.01 (0.09–0.10)	0.08 ± 0.01 (0.07–0.10)
Number of pulses of the primary note	10 ± 1.56 (8–12)	8 ± 2.57 (4–11)	18 ± 1.75 (16–20)
Pulse repetition rate of the primary note (pulses/s)	95 ± 6.42 (87–100)	66 ± 21.28 (34–77)	87 ± 2.15 (85–89)

(range 3531.4–3743.2 Hz). The difference in dominant frequency between the two species is significant (Student's t = -3.4956, df = 4.9111, p-value = 0.01788). Differences were non-significant for variation in the second component, the inter-note interval (t = -0.28265, df = 4.1541, p-value = 0.791), and for the third component, which was the duration of the primary note (t = 0.50218, df = 4.6029, p-value = 0.6386).

Principal component analysis (PCA) of advertisement calls reveals that *D. cannatellai* sp. nov. and *D. gryllatus* have low overlap in acoustic space (Fig. 3). PCA of calls from four males of *D. gryllatus* and four males of *D. cannatellai* sp. nov. yielded three components with eigenvalues > 1.0, accounting for 94% of variation (Table 4). The highest loadings for PC1 were dominant frequency of the call, dominant frequency of the primary note, and dominant frequency of the first secondary click; the highest loadings for PC2 were note duration, duration of the first secondary click, and inter-note interval; and PC3 was Duration of the primary note. *Dendropsophus cannatellai* sp. nov. differs from *D. gryllatus* primarily along PC1, which mainly represents variation in call frequency (Fig. 3A). Principal components analysis of the calls of *D. ebraccatus*, *D. cannatellai* sp. nov., and *D. gryllatus* show large acoustic divergence of the Ecuadorian species relative to *D. ebraccatus* from Central America (Suppl. material 4, figure S3).

Table 4. Character loadings, eigenvalues, and percentage of explained variance for Principal Components (PC) 1, 2 and 3 of callings of *D. cannatellai* sp. nov. and *D. gryllatus*. Bold numbers indicate highest loadings.

Variable	**Character Loading**		
	PC1	**PC2**	**PC3**
Duration of the primary note	-0.1248	-0.0142	**0.8920**
Duration of the first secondary click	0.3392	**0.4866**	-0.2024
Pulse duration of the primary note	-0.4004	0.3719	**0.2348**
Dominant frequency of the call	**-0.4726**	0.1684	-0.1542
Dominant frequency of the primary note	-0.4707	0.1436	-0.1944
Dominant frequency of the first secondary click	**-0.4715**	0.0539	-0.1824
Inter-note interval	-0.2044	**-0.7568**	-0.1157
Eigenvalue	2.0372	1.1265	1.0557
Explained variance	59.29%	18.13%	15.92%

We also describe the advertisement (Fig. 4) and aggressive calls (Fig. 5) of *D. cannatellai* sp. nov. and compared it to the calls of *D. gryllatus* and *D. ebraccatus*.

The call's acoustic parameters are summarized in Table 3. The basic call structure includes a primary note followed by a secondary click (Fig. 4A). The primary note is a sequence of pulses with a mean pulse repetition rate of 95 pulses per second (SD = 6.42). This primary note typically lasts 0.11 seconds (mean = 0.11 s, SD = 0.02) and has ~10 pulses. The first secondary click, a short burst with minimal amplitude modulation, has a duration of about 0.03 seconds (mean = 0.03 s, SD = 0.01). The power spectrum shows an average dominant frequency of the call of 3274.74 Hz (Fig. 4C), with a standard deviation of 155.74 Hz.

The average dominant frequency of the primary note was 3294.93 Hz (SD = 142.00), while the first secondary click averaged 3255.37 Hz (SD = 188.38). The average inter-note interval between primary notes is 0.09 seconds (SD = 0.01).

We analyzed calls of *D. ebraccatus* from Mexico, Guatemala, and Panama, and averaged them across regions. When compared to its sister species, *D. gryllatus* and *D. ebraccatus*, *D. cannatellai* exhibits notable differences. The duration of the primary note in *D. gryllatus* is similar to *D. cannatellai*, averaging 0.11 seconds (SD = 0.01), but *D. ebraccatus* has a significantly longer primary note duration of 0.21 seconds (SD = 0.02). The first secondary click is shorter in *D. gryllatus* (0.03 ± 0.02 s), comparable to *D. cannatellai*, but longer in *D. ebraccatus* at 0.05 seconds (SD = 0.01).

Dendropsophus gryllatus has a higher mean dominant frequency at 3606.80 Hz (SD = 93.44) vs. *D. ebraccatus* 2386.23 Hz (SD = 1218.38). The dominant frequency of the primary note in *D. gryllatus* is also higher (3604.13 ± 77.28 Hz) compared to *D. cannatellai*, while *D. ebraccatus* again has a lower mean and broader range (2502.86 ± 980.60 Hz).

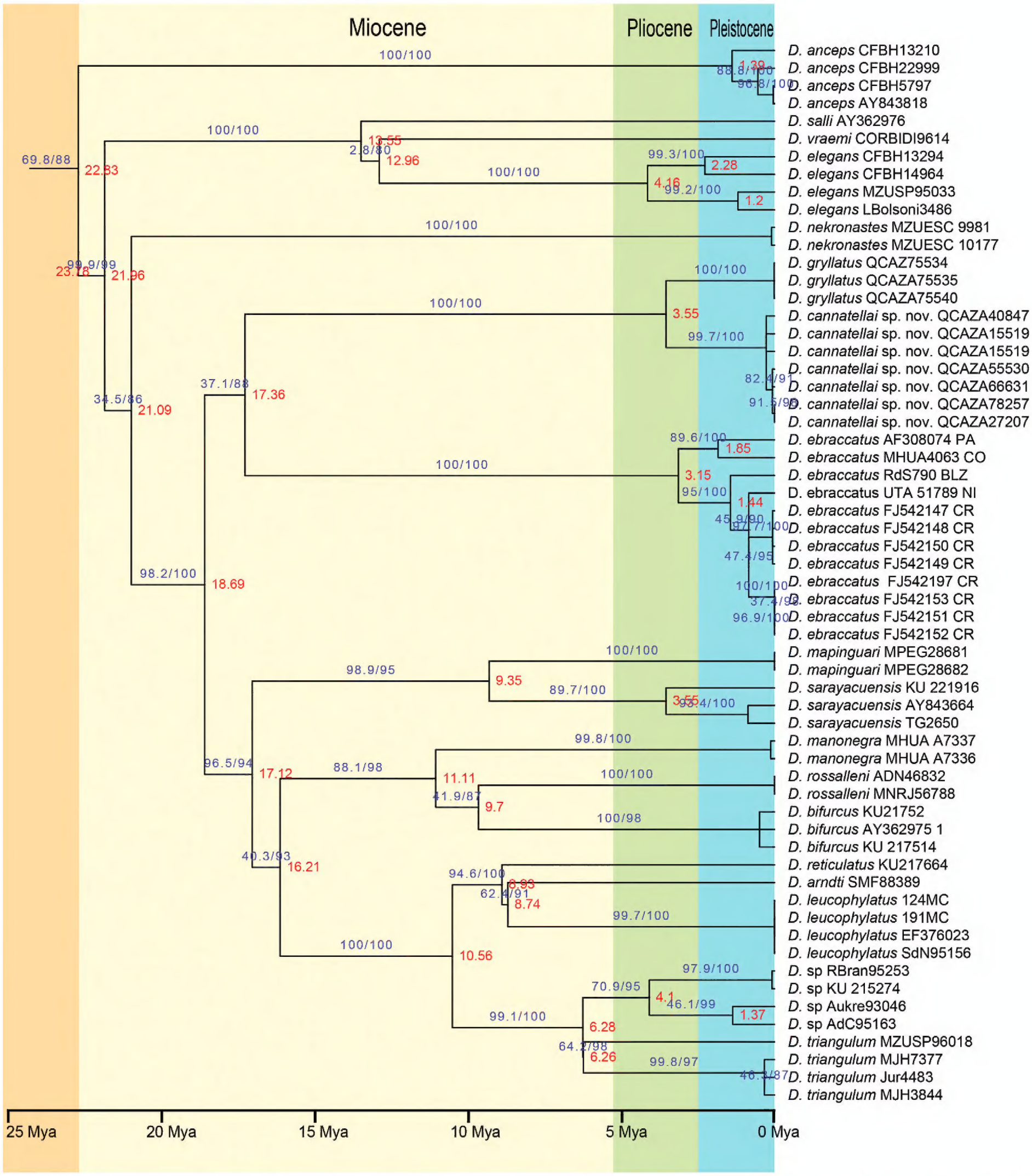

Figure 2. Chronogram of the *Dendropsophus leucophyllatus* group based on the best ML tree. Red numbers in the nodes represent divergence times in Mya; blue numbers at branches show SH-aLRT values (before slash) and ultrafast bootstrap support values (after slash). Ages less than 1 million years are not shown.

Additionally, the pulse repetition rate differs significantly among these species: *D. cannatellai* has a faster rate at 95 pulses per second, while *D. gryllatus* has a slower rate of 66 pulses per second (SD = 21.28), and *D. ebraccatus* has a slightly lower rate than *D. cannatellai* at 87 pulses per second (SD = 2.15). These variations in call structure and frequency help distinguish *D. cannatellai* from its closely related species.

Ecological niche modeling and environmental envelope

Our PCA of bioclimatic variables shows that the new species inhabits localities with warmer environmental conditions than those of *D. gryllatus* (Fig. 6). We obtained four Principal Components (PC) with eigenvalues > 1, which together explained 97% of the variation. Principal Component I explained 46.8% of the vari-

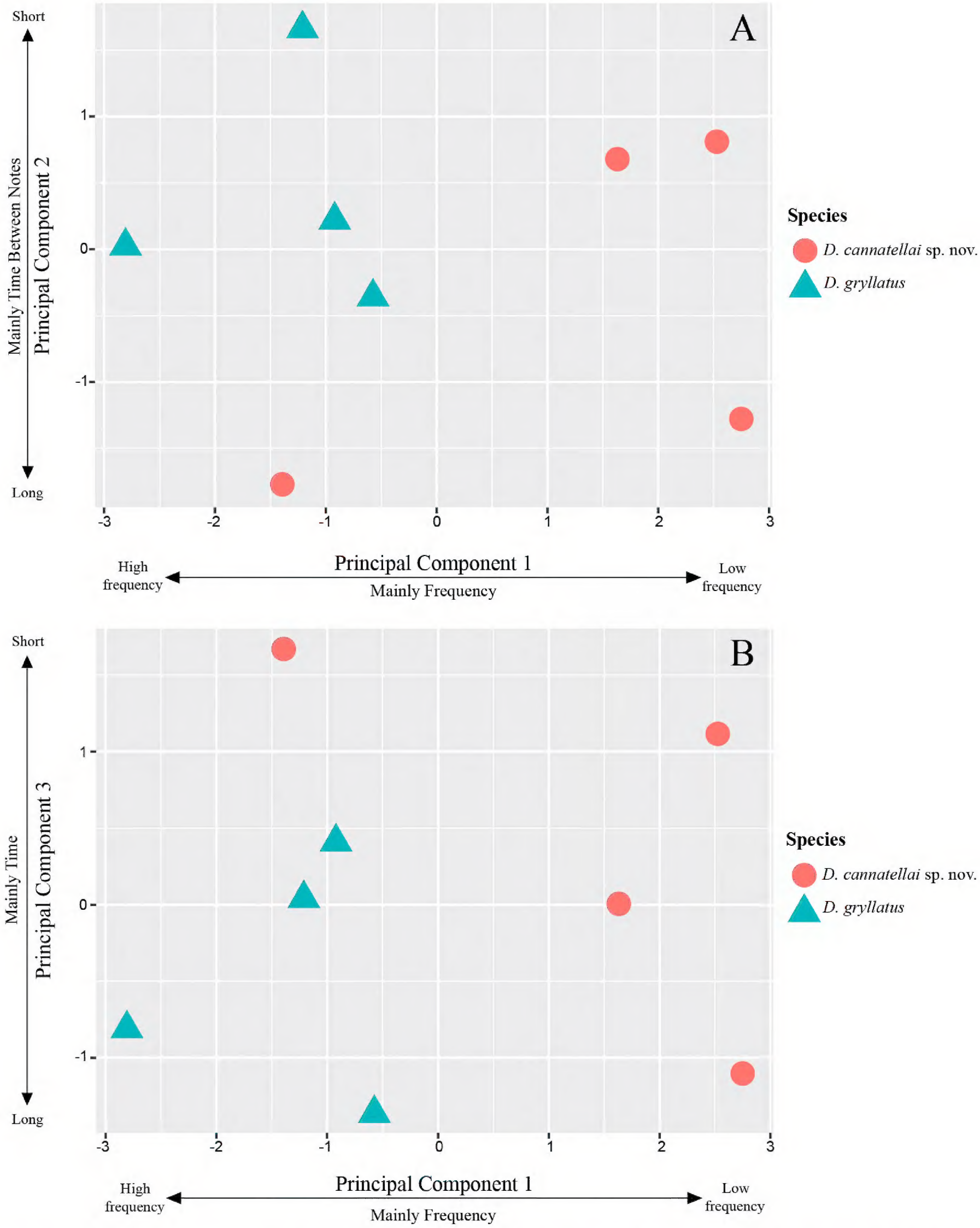

Figure 3. Principal Components Analysis based on seven acoustic variables from the advertisement calls of males of *Dendropsophus cannatellai* sp. nov. and *D. gryllatus* from western Ecuador. See Table 4 for character loadings on each component variable.

ance and had high loadings in temperature related variables (Table 5); PC II explained 33.4% of the variance and had high loadings in precipitation during the driest and coldest periods of the year (negative correlation, Table 5). We found significant differences in PC scores for PC I (Student-t = 2.452, p = 0.036) but not for PC II and PC III (Student-t PCII = 2.974, p = 0.059; PC III = 1.038, p = 0.396).

For the ecological niche model, the best model was fc.LQH_rm.2 (Linear, Quadratic, Hinge_ regularization multiplier 2) based on the average AUC with a value of 0.980 and an omission rate of 0.042. See Suppl. material 7, table S3, for the obtained models and their AUC and OR values. Fig. 7 shows the presence area for that model under the minimum training presence threshold. The presence area has ~17,000 km^2.

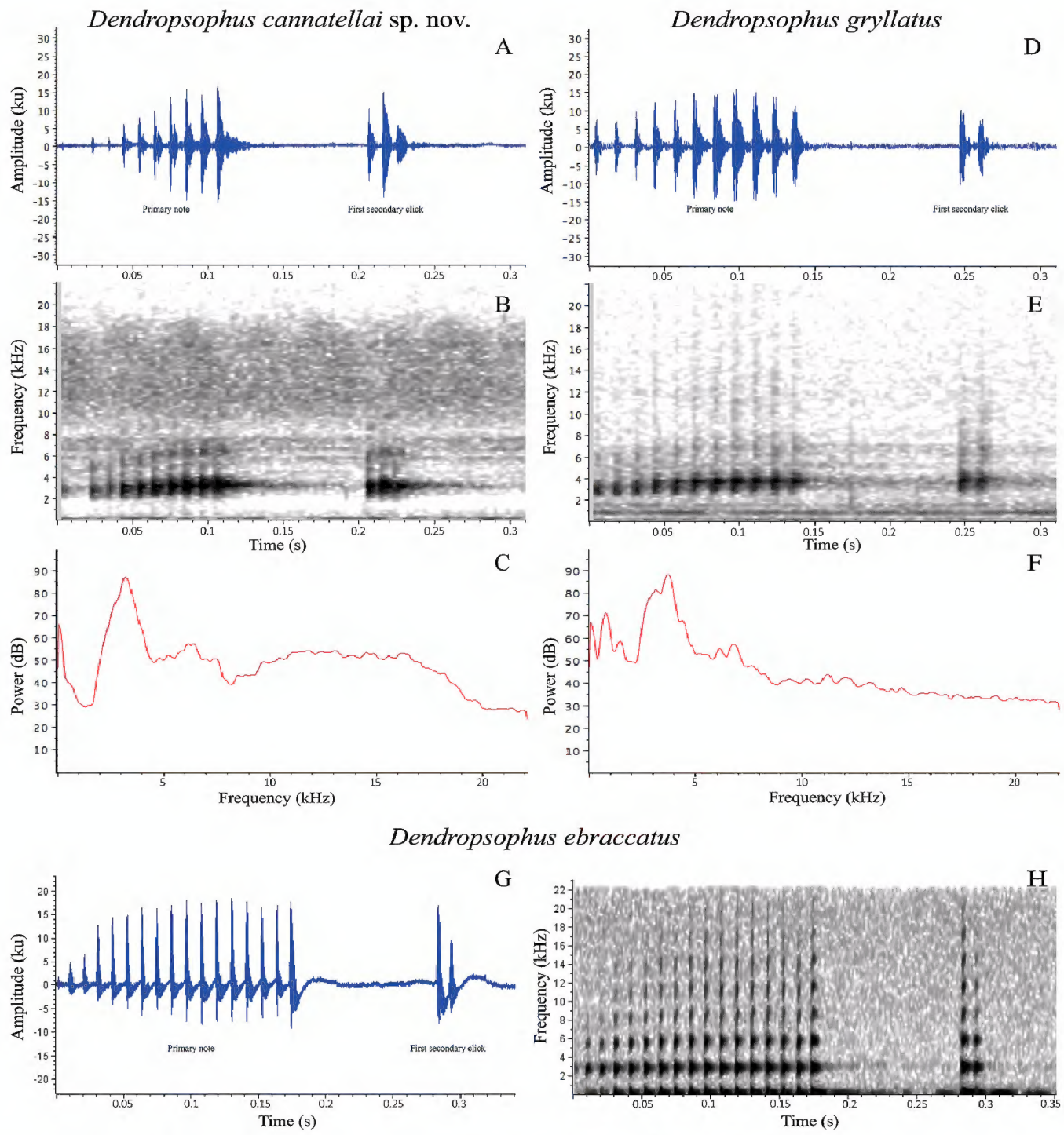

Figure 4. Advertisement calls of *Dendropsophus cannatellai* sp. nov. and *D. gryllatus* from western Ecuador, and *D. ebraccatus* sensu stricto. **A–C.** *D. cannatellai* (QCAZ 78812) from Río Silanche, Pichincha Province, Ecuador; **D–F.** *D. gryllatus* (ML 19007) from Río Palenque, Los Ríos Province, Ecuador; **G, H.** *D. ebraccatus* (ML 193729) from Toocog, Petén Department, Guatemala. **A, D** and **G** are oscillograms; **B, E** and **H** spectrograms; **C** and **F** power spectra of complete call.

Table 5. Character loadings and eigenvalues for Principal Components (PC) 1 and 2 of bioclimatic variables of *Dendropsophus cannatellai* sp. nov. and *D. gryllatus*. Bold characters indicate highest loadings.

Variable	Character Loading		
	PC1	PC2	PC3
Annual mean temperature	0.3041	0.1010	0.2154
Average monthly temperature range	-0.2514	0.1899	0.0992
Isothermality (BIO2/BIO7)	0.1228	-0.2611	0.2548
Temperature seasonality (Std. Dev * 100)	-0.0876	0.2067	**0.4328**
Maximum temperature of the warmest month	0.1264	0.2900	0.2373
Minimum temperature of the coldest month	**0.3240**	-0.0625	0.0439
Annual temperature range (BIO5-BIO6)	-0.2501	0.2078	0.0826
Mean temperature of the wettest trimester	0.2992	0.1061	0.2338
Mean temperature of the driest trimester	**0.3149**	0.0813	0.1666
Mean temperature of the warmest trimester	0.2951	0.1165	0.2411
Mean temperature of the coldest trimester	**0.3100**	0.0974	0.1799
Annual precipitation	-0.1048	-0.3401	0.2561
Precipitation of the wettest month	-0.2451	-0.1482	**0.3611**
Precipitation of the driest month	0.0812	**-0.3743**	0.0069
Precipitation seasonality (CV)	-0.2235	0.2811	0.1098
Precipitation of the wettest trimester	-0.2470	-0.1436	**0.3583**
Precipitation of the driest trimester	0.0950	**-0.3716**	0.0119
Precipitation of the warmest trimester	-0.2369	-0.1748	0.3419
Precipitation of the coldest trimester	0.1118	**-0.3531**	0.0078
Eigenvalue	2.9847	2.5199	1.5270

Systematic account

Dendropsophus cannatellai sp. nov.

https://zoobank.org/21322A55-F753-4BBA-A109-732F92DA33A5

Dendropsophus ebraccatus: Ortega-Andrade et al. 2010.
Dendropsophus ebraccatus: Ron et al. 2011.
Dendropsophus ebraccatus: Simpson et al. 2013.
Dendropsophus ebraccatus: Caminer et al. 2017.
Dendropsophus ebraccatus (in part): Pirani et al. 2020.
Dendropsophus ebraccatus (in part): Orrico et al. 2021.
Dendropsophus ebraccatus: Pintanel et al. 2022.
Dendropsophus ebraccatus (in part): Touchon et al. 2024.

Holotype. • QCAZ 40847 (field no. SC-PUCE 19751), adult male from Ecuador, Esmeraldas Province, Cantón San Lorenzo, Playón San Francisco (1.0873°N, 78.6905°W), 64 m, collected by Luis A. Coloma, Santiago R. Ron, and Mark Weiner on 06 August 2007.

Paratypes (130): All specimens were collected in Ecuador. Pichincha Province: • QCAZ 3768–3774, 4840–4843 Cantón Pedro Vicente Maldonado, 1 km E from Maldonado (0.0832°N, 79.0394°W), 745 m, collected by

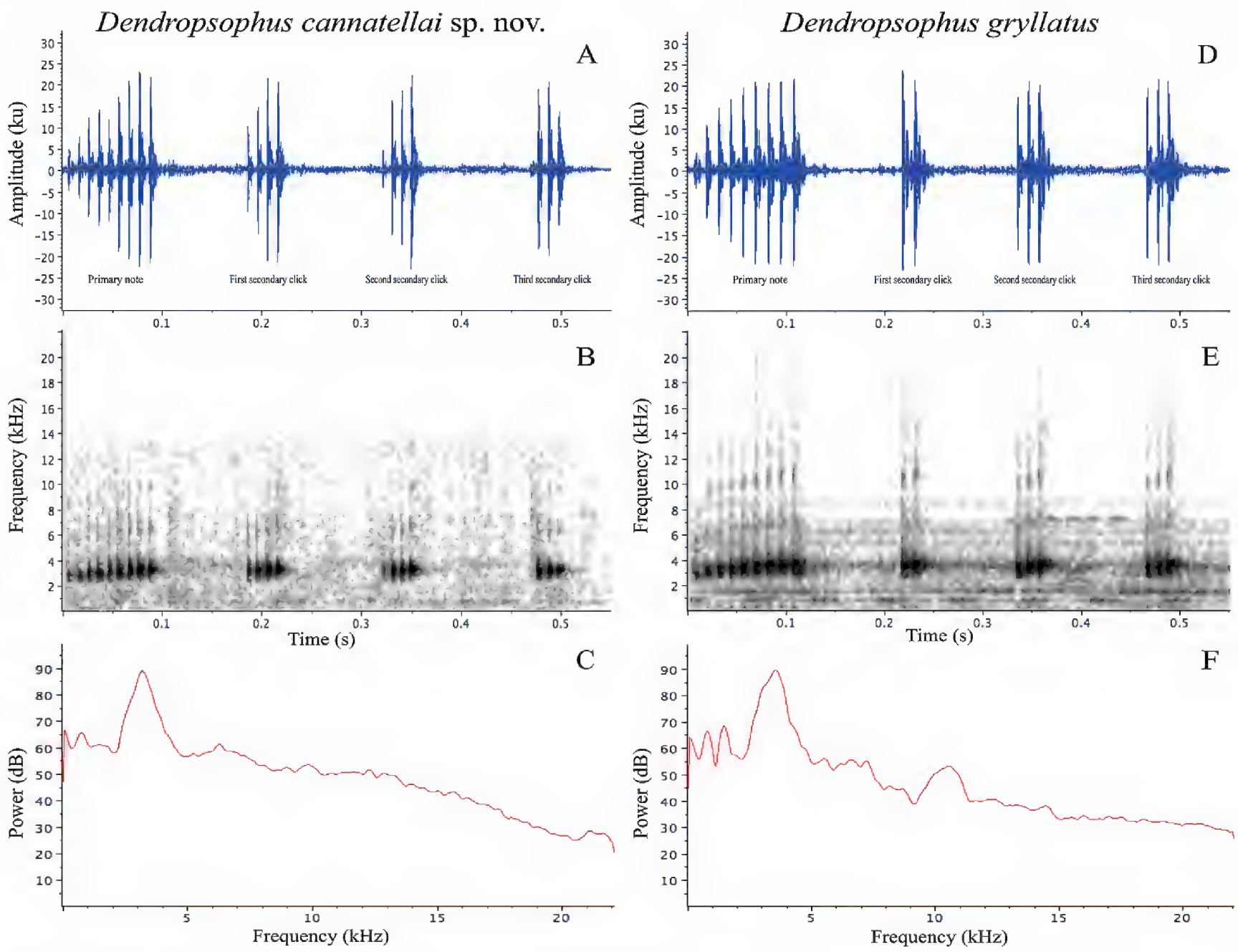

Figure 5. Aggressive calls of *Dendropsophus cannatellai* sp. nov. and *D. gryllatus* from western Ecuador. **A–C.** *D. cannatellai* sp. nov. (QCAZ 78812) from Río Silanche, Pichincha Province, Ecuador; **D–F.** *D. gryllatus* (ML 19006) from Río Palenque, Los Ríos Province, Ecuador. **A** and **D** are oscillograms; **B** and **E** spectrograms; **C** and **F** power spectra of complete call.

Stephan Lötters and Luis A. Coloma on 13 March, 1993; • QCAZ 9457, 9489, Cantón Pedro Vicente Maldonado, Río Pitzará (0.1192°N, 79.2344°W), 280 m, collected by Giovanna Rodríguez on 01 January, 1996 and 01 August, 1995; • QCAZ 10434, 27207–27209 Cantón Puerto Quito, Aldea Salamandra (0.1192°N, 79.2344°W), 149 m, collected by David Cannatella on 08 April, 2004; • QCAZ 27623–27624 Cantón Pedro Vicente Maldonado, 1 km E from Maldonado (0.0829°N, 79.0383°W), 670 m, collected by John J. Wiens on 30 March, 1990; • QCAZ 78254–78259, 78309, 78576 Cantón Pedro Vicente Maldonado, Río Silanche (0.1278°N, 79.1414°W), 369 m, collected by Gabriela B. Bittencourt on 19 January, 2023; • QCAZ 78809–78814 Cantón Pedro Vicente Maldonado, Río Silanche (0.1278°N, 79.1414°W), 369 m, collected by Santiago R. Ron on 17 July, 2023. Esmeraldas Province: Santo Domingo de Onzole (0.8003°N, 79.0709°W), 110 m, collected by Néstor Acosta on 18 January, 1997; • QCAZ 10704, 22893, Cantón Pedro Vicente Maldonado (0.0878°N, 79.0491°W), 670 m, collected by Luis Coloma on 13 March, 1993 and Sebastián Valdiviezo on 31 March, 1990. Esmeraldas Province: • QCAZ 15519, 23156, 23160, 23371, Cantón San Lorenzo, 3 km west of Durango (1.0643°N, 78.6443°W), 158 m, collected by Ítalo Tapia on 15 June, 2001 and David Cannatella on 03 March, 2003; • QCAZ 23162 Cantón San Lorenzo, Durango (1.0127°N, 78.8954°W), 14 m, collected by David Cannatella on 04 March, 2003; • QCAZ 26098, 26100 Cantón San Lorenzo, Durango – San Lorenzo (1.0793°N, 78.6695°W), 74 m, collected by Néstor Acosta on 08 June, 2003; • QCAZ 29489–29511, 30329–30330, 55529–55530 Cantón San Lorenzo, Durango (1.0427°N, 78.6244°W), 85 m, collected by Ítalo Tapia on 02 February, 2005, Elicio Tapia on 19 December, 2004 and Justin Touchon on 20 April, 2013; • QCAZ 29799–29809, 30255 Cantón San Lorenzo, Durango – San Francisco (1.0872°N, 78.6905°W), collected by Ítalo Tapia on 17 September, 2004; • QCAZ 32136 San Francisco, 1.3 km east (1.0888°N, 78.69563°W), 85 m, collected by Diego Almeida on 26 May, 2006; • QCAZ 35709–35710 La Mayronga (1.05°N, 79.27°W), 150 m, collected on 27 November, 1998; • QCAZ 37741, 37845 Cantón San Lorenzo, 21 km of Durango (1.0248°N, 78.6175°W), 284 m, collected by Ítalo Tapia on 03 January, 2008; • QCAZ 37749 Cantón San Lorenzo, 21 km of Durango (1.0470°N, 78.6182°W), 104 m, collected by Ítalo Tapia on 15 December, 2007; • QCAZ 40276, 40279 Cantón San Lorenzo, 2 km east of Durango (1.0247°N, 78.6174°W), 85 m, collected by Ítalo Tapia on 13 March, 2009; • QCAZ 51854, 51863, 51877 Cantón San Lorenzo, Durango (1.0379°N, 78.6222°W), 283 m, collected by Andrés Merino on 10 September, 2011; • QCAZ 55531–

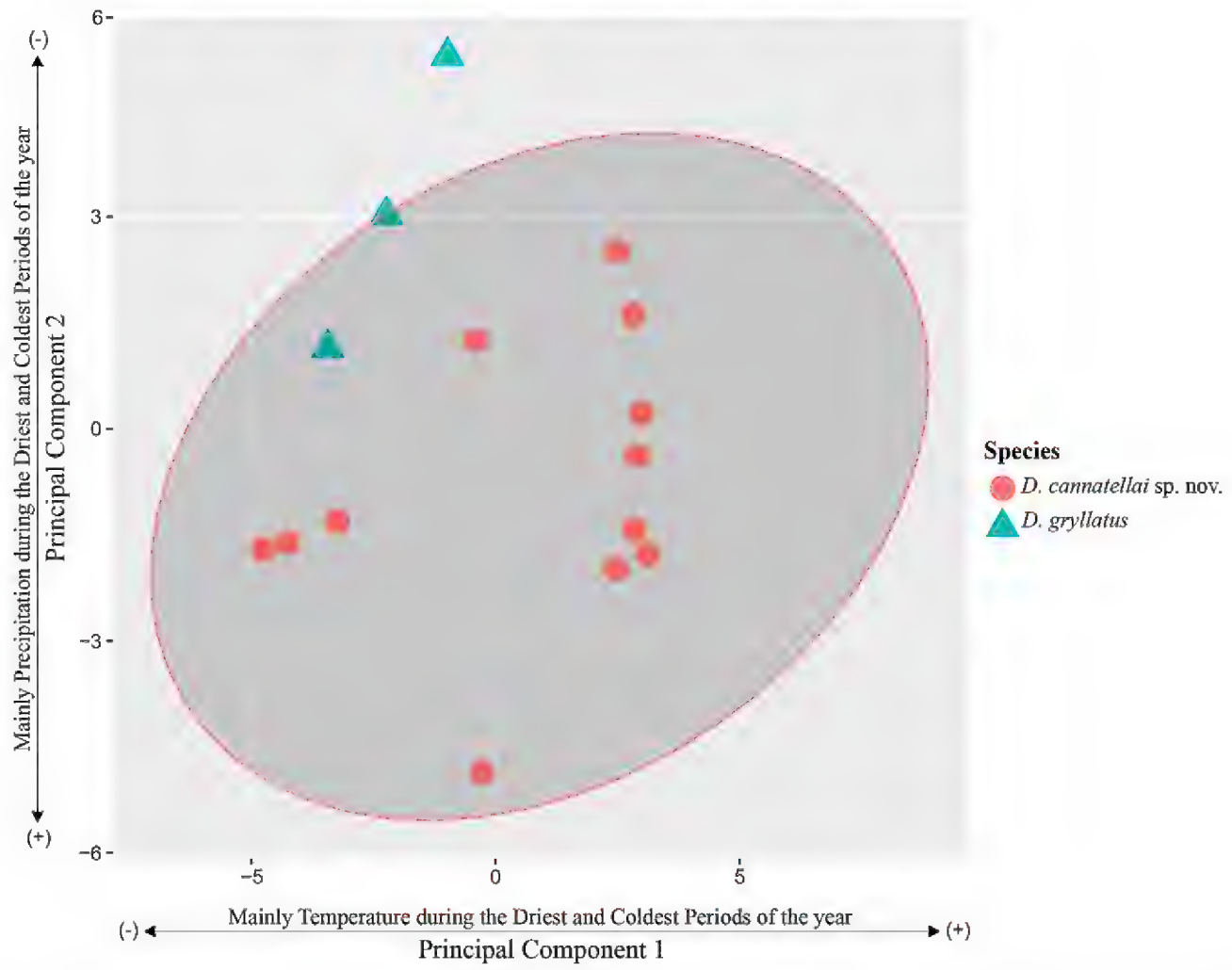

Figure 6. Principal Component Analysis of 19 bioclimatic variables for localities of *D. cannatellai* sp. nov. and *D. gryllatus*. The ellipses show the 95% confidence level for *D. cannatellai* sp. nov.

540, 55545–55550, 55555–55558 Cantón San Lorenzo, 9 km west of Durango (1.2083°N, 78.7413°W), 91 m, collected by Justin Touchon on 26 April, 2013; • QCAZ 55541–55544, 55551–55554 Cantón San Lorenzo, 7 km west of Durango (1.2044°N, 78.8447°W), 139 m, collected by Justin Touchon on 22 April, 2013; • QCAZ 66629–66635 Cantón San Lorenzo, Durango (1.0874°N, 78.6221°W), 265 m, collected by Diego Almeida on 10 February, 2017.

Common names. English: Cannatella's treefrog. Spanish: Ranita de Cannatella.

Definition (Figs 8, 9). In this section, we describe coloration in life. We assign the new species to the genus *Dendropsophus* based on the phylogeny (Fig. 1). The new species is characterized by: (1) mean SVL 23.4 mm in males (range 21–26; n = 115); 30.7 mm in females (range 28–33; n = 14); (2) axillary membrane reaching arm halfway to elbow; (3) reduced webbing on fingers; (4) webbing on feet; (5) palmar tubercle single; (6) pectoral glands present; (7) dorsal background coloration brown with white to bright yellow dorsolateral bands, extending to the eyes and top of head; white or bright yellow well defined sacral mark, fused with dorsolateral bands in some individuals; (8) absence of a light labial stripe in contact with the orbit; (9) dorsal surfaces of the limbs brown, with white to bright yellow ovoid marks, with the forearm typically bearing one to two marks, and the shank one to three; (10) webbing and ventral surfaces vary from orange to yellow; (11) iris dull bronze to coppery bronze, and (12) advertisement call pulsed with a mean dominant frequency = 3274.7 Hz (range 3169.0–3498.7) and mean pulse rate of the primary note = 95 pulses/s (range 87–100).

Figure 7. Habitat suitability prediction of *D. cannatellai* sp. nov. based on the fc.LQH_rm.2 model. Purple area represents the area of possible presence of the species.

Figure 8. Life coloration of *Dendropsophus cannatellai* sp. nov. First and third rows, dorsolateral views; second and fourth, ventral views. From left to right, first and second rows: QCAZ 51877 (SVL = 22.26 mm, male); QCAZ 78809 (SVL = 33.61 mm, female); QCAZ 55558 (SVL = 21.96 mm, male); third and fourth rows: QCAZ 40847 (holotype; SVL = 22.32 mm, male); QCAZ 78812 (SVL = 25.86 mm, male); QCAZ 78813 (SVL = 24.94 mm, male). See type series for locality data. All specimens are shown at the same scale.

Diagnosis. In this section, coloration refers to live adult individuals, unless otherwise noted. Adult individuals of *Dendropsophus cannatellai* sp. nov. can be distinguished from other species of the genus *Dendropsophus* that do not belong to the *D. leucophyllatus* group by the presence of two pectoral glands. Within the *D. leucophyllatus* group, we focus our comparisons with species from Central America and the Chocó region, also the most closely related. Other species of the group have a cis-Andean distribution and, therefore, cannot be confused with the new species. Nevertheless, we include diagnosis for species from the western Amazon basin, which are geographically closest to the new species range.

Dendropsophus ebraccatus differs from the new species (characters of the later in parenthesis) in having a light labial stripe reaching the orbit (area below the eye has dark background color, sometimes with one or two small light spots). In addition, *D. ebraccatus* either lacks dorsolateral yellow bands or, if present, they are wide and sinuous (if present, yellow dorsolateral bands straight to moderately curved; variation in coloration of *D. ebraccatus* from Duellman 1970 and Ohmer et al. 2009).

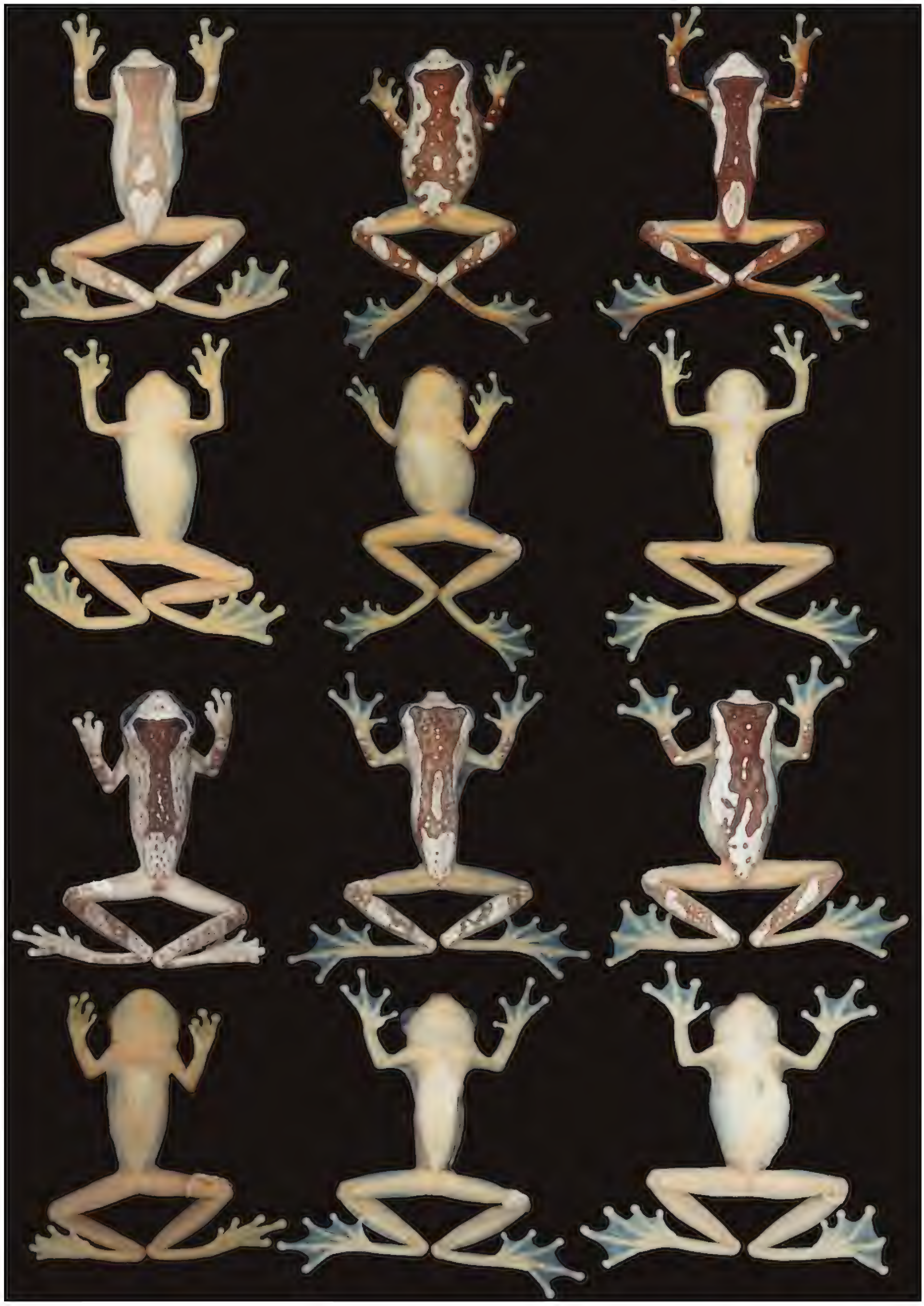

Figure 9. Adult preserved specimens of *Dendropsophus cannatellai* sp. nov. First and third rows, dorsolateral views; second and fourth, ventral views. From left to right, first and second rows: QCAZ 9457 (SVL = 28.65 mm, female); QCAZ 23162 (22.83 mm, male); QCAZ 26098 (30.73 mm, female); third and fourth rows: QCAZ 35710 (24.74 mm, male); QCAZ 78254 (24.71 mm, male); QCAZ 78257 (31.94 mm, female). See type-series for locality data. All specimens are shown at the same scale.

Figure 10. Tadpole (QCAZ 78576) of *Dendropsophus cannatellai* sp. nov, stage 25 (Gosner 1960). Dorsal, ventral, and lateral views. Body length = 8.14 mm; tail length = 16.24 mm; total length = 24.38 mm.

Dendropsophus cannatellai sp. nov. clearly differs from its sister species, *D. gryllatus*, in dorsal coloration and by being larger (although SVL ranges overlap: male average SVL = 21.95, range 18.71–24.69 mm vs. SVL = 23.43, range 21.05–26.58 mm in *D. cannatellai* sp. nov.) The dorsal pattern of *D. gryllatus* consists of two longitudinal dark brown lines against a pale-yellow background (Fig. 14; brown background with clear yellow dorsolateral bands in the new species). The new species also differs from *D. gryllatus* by having bright orange flash coloration (pale yellow in *D. gryllatus*). *Dendropsophus gryllatus* exhibits a sacral spot that extends forward, making it more elongated and continuous with other dorsal markings (the sacral spot of *D. ebraccatus* is distinct, circular or slightly oval, and symmetrically positioned near the lower back, with well-defined edges that contrast against its darker dorsal pattern; sacral spot is absent in some individuals).

The Amazonian species *D. sarayacuensis* and *D. bifurcus* also has a brown background color with yellow bands and marks. However, *D. sarayacuensis* differs in that the yellow areas in the shanks have irregular borders (borders are more linear in *D. cannatellai* sp. nov.) *Dendropsophus bifurcus* differs by having less extensive yellow bands and marks, especially in the shanks where, in most individuals, they are absent, except for the heel (extensive yellow marks along the shank in *D. cannatellai*). *Dendropsophus reticulatus* differs by having a uniform clear dorsal color pattern, sometimes with one or several dark brown round marks (Caminer et al. 2017) (clear dorsal pattern restricted to head, dorsolateral bands, and rump in *D. cannatellai*). *Dendropsophus triangulum* and *D. arndti* differ by being larger, SVL > 28.0 mm in males and > 33.0 mm in females (Caminer et al. 2017) (*D. cannatellai* males SVL range 21.05–26.58 mm, females = 28.25–31.94 mm).

Dendropsophus cannatellai sp. nov. can be distinguished from *Dendropsophus carnifex* (*D. columbianus* group), a species from the Andean Chocó, by having a short axillary membrane that reaches halfway to the elbow (axillary membrane absent in *D. carnifex*).

Description of holotype (Figs 12, 13). Adult male, SVL 22.32 mm, foot length 3.04 mm, head length 7.42 mm, head width 7.58 mm, eye diameter 3.34 mm, tympanum diameter 1.25 mm, tibia length 11.8 mm, femur length 10.88 mm, arm length 4.55 mm, eye-nostril distance 1.66 mm. Body as wide as head, head wider than long; snout short, truncated in dorsal view and profile; distance from nostril to eye shorter than eye diameter; canthus rostralis barely distinct, rounded; loreal region slightly concave; internarial area subtly depressed; nostrils slightly protruding, directed posterolaterally; interorbital region flat; eyes large, prominent; eye diameter 2.7 times tympanic annulus diameter; tympanum hidden beneath skin; tympanic membrane absent, tympanic annulus visible under skin, oval, longer dorsoventrally and concealed dorsally by supratympanic fold, separated from eye by about 57% of its diameter; faint supratympanic fold, extending posteriorly from rear corner of eye to anterior edge of arm insertion. Arm sturdy and short, axillary membrane extends halfway to elbow; relative length of fingers I < II < IV < III; fingers with large rounded discs, that of Finger III approximately the same diameter as tympanum; subarticular

Figure 11. Metamorph, juvenile and subadults of *Dendropsophus cannatellai* sp. nov. Dorsolateral views of individuals raised in captivity in Balsa de los Sapos. From left to right, first row: QCAZA l 78576 (total length = 23.27 mm); QCAZA n 79747 (SVL = 11.57 mm); second row: (18.46 mm); (19.59 mm); third row: (19.38 mm); (17.89 mm). All subadults approximately 1 year old since hatching.

tubercles prominent, round, subconical, single; distal tubercle on Finger IV bifid; supernumerary tubercles present; palmar tubercle indistinct; prepollex sharp-pointed (based on x-ray image); nuptial excrescences absent; hand webbing formula I basal II1 ½ — 2 ½ III 2 ⅔ — 2 IV. Hindlimbs large; toes with discs slightly wider than long, smaller than those on fingers; relative toe length I < II < V < III < IV; outer metatarsal tubercle indistinct, small, round; inner metatarsal tubercle large, elongated, elliptical; subarticular tubercles single, round, flat; supernumerary tubercles limited to soles, small; foot webbing formula I1+ —2II1+ —2–III1+ —2IV2+ —1+ V (Fig. 11). Two pectoral glands bellow the insertion of the arms, separated from each other by about half their individual width. Skin on dorsum, head, flanks, and dorsal surfaces of limbs smooth. Ventral skin coarsely granular, except for pectoral glands, which are finely granular. Ventral surfaces of body and thighs granular. Longitudinal wrinkles of vocal sac from throat to front of the insertion of the arms.

Figure 12. Dorsal, ventral and lateral views of the holotype of *Dendropsophus cannatellai* sp. nov. (QCAZ 40847, SVL 22.32 mm).

Skin on arms and shanks smooth. Cloacal opening directed posteriorly at upper level of the thighs, covered by a long, broad cloacal sheath. Tongue broadly heart-shaped, free laterally and posteriorly, widely attached to mouth floor. Vomerine teeth between choanae, in two slightly angled rows, not contacting each other, smaller than ovoid choanae. In life dorsal background coloration is brown with yellow dorsolateral bands, extending to the eyes and top of head (Fig. 8); bright yellow well defined sacral mark; absence of a light labial stripe and large suborbital mark; the dorsal surfaces of the thighs is light brown; the forearm and shank have two yellow transversal marks each; coloration of webbing and ventral surfaces yellow; iris coppery bronze. Color of holotype in preservative shown in Fig. 12.

Variation. Sexual dimorphism is observed in the size of adult individuals, where males are smaller (SVL males = 21.05–26.58 mm; SD = 1.235. SVL females = 28.25–31.94 mm; SD = 2.078).

Color variation in life and preservative is shown in Figs 8, 9. In some individuals (e.g., QCAZ 55555) the dorsolateral bands are extensive and fused with the sacral mark. There is variation in the extent of membrane between the digits of the forelimbs, particularly between fingers II, III, and IV, where adult females have more extensive membrane. In dorsal view, snout shape varies from truncate to slightly rounded. In preserved male specimens, the vocal sac is evident as wrinkles in the gular region. However, in some individuals, these wrinkles are less noticeable.

Distribution, natural history, and conservation status. *Dendropsophus cannatellai* sp. nov. occurs in Western Foothill Forest and the Chocó Tropical Rainforest in NW Ecuador and SW Colombia. Although the occurrence in Colombia needs to be corroborated, we found the following evidence of its presence: (1) localities in Ecuador near the border with Colombia, and (2) records on iNaturalist (observation numbers 147931034 in Tumaco, Nariño, and 36196673 in San Andrés de Tumaco), morphologically indistinguishable from the new species.

Within its distribution range, climatic conditions are generally warm and humid, with an annual average temperature ranging from 22.5 to 25.4 °C and an average annual precipitation with a range from 1025 to 3348 mm. The physiognomy of these ecosystems consists of big trees that can reach almost 30 m tall, and a great abundance of palms. The Western Foothill Forest has an elevation range from 300 to 1300 m, with a dominance of plants from the families Mimosaceae, Fabaceae, and Burseraceae with a high percentage of endemism. The presence of epiphytes is common. The Chocó Tropical Rainforest has an elevation from 0 to 300 m, with an abundance of ferns and a high diversity of trees (Ron et al. 2024).

The new species is found in artificial open areas, near ponds and puddles where herbaceous vegetation is abundant. It is less frequent in secondary forest. Males call from leaves or grasses less than 2 m above water, between the 18:00 and 0:00 hours. A couple collected in Río Silanche, laid a clutch in captivity with 190 eggs. Experiments in captivity report average clutch sizes of 84 eggs

Figure 13. Ventral views of the holotype's hand (left) and foot (right) of *Dendropsophus cannatellai* sp. nov. (QCAZ 40847).

under shaded conditions and 98 under unshaded conditions (Touchon et al. 2024). In the same experiments, most females laid terrestrial eggs, but 30% of females laid a few eggs in water, under unshaded conditions.

The new species is assigned to the Red List category Near Threatened (NTU). Its extent of occurrence (EOO) has < 20000 km^2 (minimum convex polygon of the known localities of *D. cannatellai* sp. nov. ~6134 km^2). However, populations are predominantly located on disturbed and deforested areas, near roads. The species appears to thrive in human modified habitats including pastures for cattle raising and ponds in artificial open areas with abundant herbaceous vegetation.

Etymology. The specific name *cannatellai* is a noun in the genitive case and is a patronym for David C. Cannatella, who collected type specimens of the new species. Moreover, during his career he has contributed extensively to the study of systematics and evolution of neotropical amphibians. He has been integral part of scientific societies, exemplified by his presidencies of the American Society of Ichthyologists and Herpetologists (2002–2003) and the Society of Systematic Biologists (2004–2005). Currently he is Dean of the Department of Integrative Biology at the University of Texas at Austin, USA.

Discussion

Our data, in combination with previous publications (Pirani et al. 2020; Orrico et al. 2021), shows convincingly that the Ecuadorian populations previously identified as "*Dendropsophus ebraccatus*" represent a new species from the Chocó region of Ecuador and SW Colombia. Evidence of the distinctiveness of both species is based on mitochondrial DNA and RAD-Seq data published by Pirani et al. (2020), who found two alternative topologies for the position of *D. ebraccatus* and *D. cannatellai* sp. nov.: (1) as sister species (consistent with our topology; they did not include *D. gryllatus*), and (2) paraphyletic, with *D. cannatellai* sp. nov. sister to a clade of four Amazonian species and *D. ebraccatus* sister to them. Either topology had low support, both in our tree and in those of Pirani et al. (2020). Evidence of paraphyly and the > 10 My divergence between *D. cannatellai* sp. nov. and *D. ebraccatus* indicate that they are, in fact, separate species (see also Pirani et al. 2020). Those results are corroborated by our mitochondrial tree and morphological comparisons.

The application of the binomen *Hyla ebraccata* to the Central American clade is based on the location of its type locality "region of Nicaragua" (Cope 1874). An available junior synonym for *Dendropsophus ebraccatus*, *Hyla weyerae* Taylor 1854, has its type locality in Puntarenas Province, Costa Rica, which also overlaps with the Central American Clade. Within the Central American clade, we found two seemingly allopatric subclades with a divergence time estimate of ~3 My. The western subclade is distributed in Belize, Nicaragua, and Costa Rica; the eastern subclade is distributed in northern Colombia and Panama. Recently published genomic data for Central American populations also indicate deep divergences among regions (Touchon et al. 2024). If each subclade represents

Figure 14. Life coloration of *Dendropsophus gryllatus*. First and third rows, dorsolateral views; second and fourth, ventral views. From left to right, first and second rows: QCAZ 75534 (SVL = 20.80 mm); QCAZ 75535 (SVL = 21.19 mm); QCAZ 75536 (SVL = 22.24 mm); third and fourth rows: QCAZ 75538 (SVL = 18.71 mm); QCAZ 75539 (SVL = 21.89 mm); QCAZ 75540 (SVL = 20.26 mm); all adult males. See Suppl. material 1, table S1 for locality data. All specimens are shown at the same scale.

a separate species, the binomens *Hyla ebraccata* and *Hyla weyerae* should correspond to the western subclade leaving the eastern subclade as an undescribed species.

The available evidence indicates that *D. cannatellai* sp. nov. and *D. ebraccatus* are allopatric. Therefore, all GenBank sequences previously ascribed to "*D. ebraccatus*" from Ecuador, actually belong to *D. cannatellai* sp. nov. They were published by Caminer et al. (2017) and Touchon et al. (2024). Sequences by Touchon et al. (2024) from Central America as well as all sequences published by Ohmer et al. (2009) and Robertson et al. (2009) belong to *D. ebraccatus*.

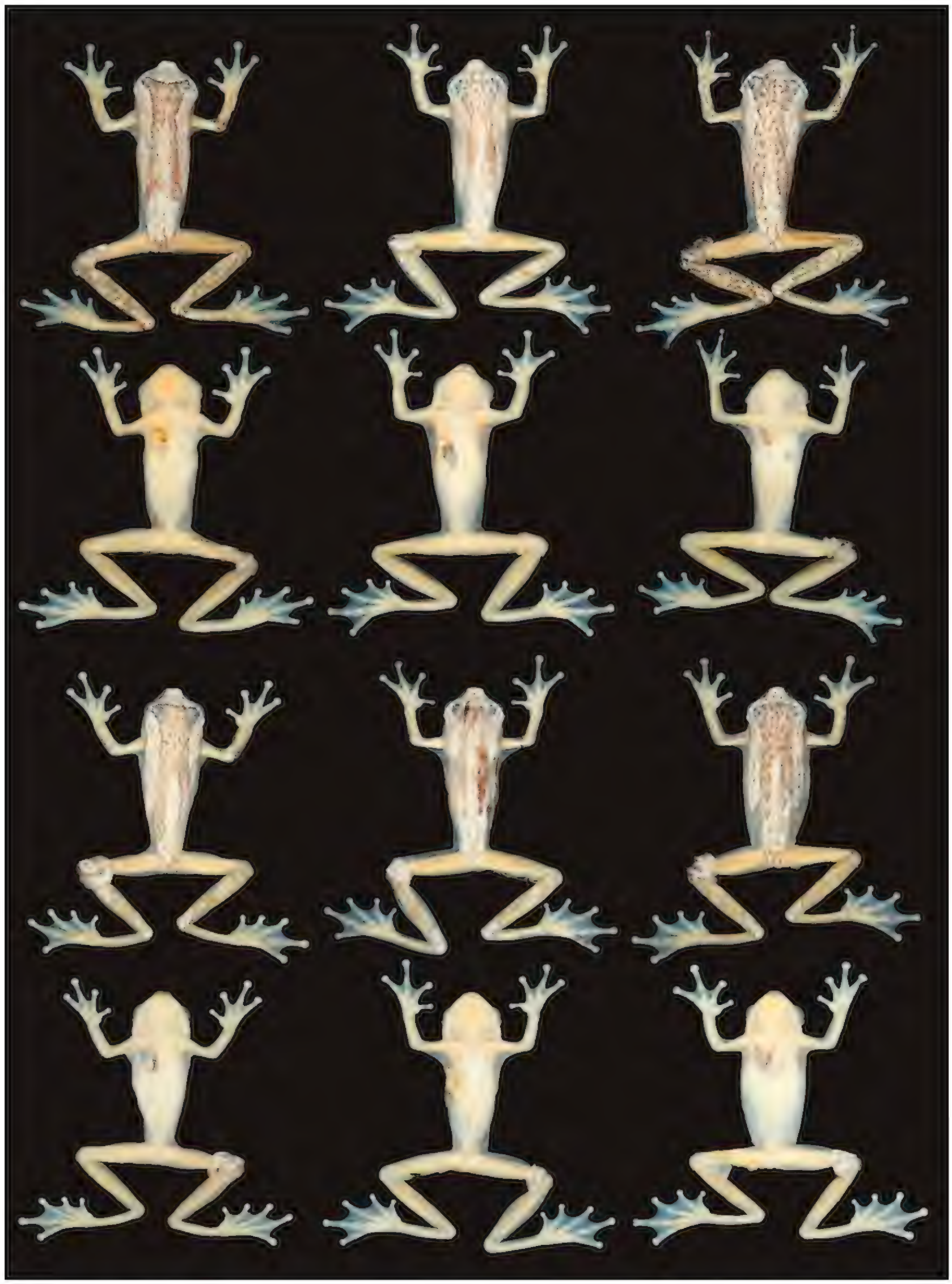

Figure 15. Adult preserved specimens of *Dendropsophus gryllatus* showing variation in dorsal and ventral coloration. From left to right, first and second rows: QCAZ 75532 (22.54 mm); QCAZ 75533 (21.96 mm); QCAZ 75535 (21.19 mm); third and fourth rows: QCAZ 75536 (22.24 mm); QCAZ 75537 (22.85 mm); QCAZ 75539 (21.89 mm); all adult males. See Suppl. material 1, table S1 for locality data. All specimens are shown at the same scale.

We report, for the first time, the phylogenetic position of *D. gryllatus*, one of the few species of *Dendropsophus* of unknown evolutionary affinities (Orrico et al. 2021). Its inclusion in phylogenetic studies was precluded by its scarcity in the field, with only few known localities in Ecuador (Fig. 14). In its description, Duellman (1973) considers *D. gryllatus* part of the "*H. microcephala*" species group. Although he noted that its color pattern is reminiscent of *D. ebraccatus* and *D. triangulum* (reported by him as "*D. leucophyllata*"), he rejected a close relationship with them arguing that *D. gryllatus* have less extensive axillary membrane and absence of glands on the pectoral region.

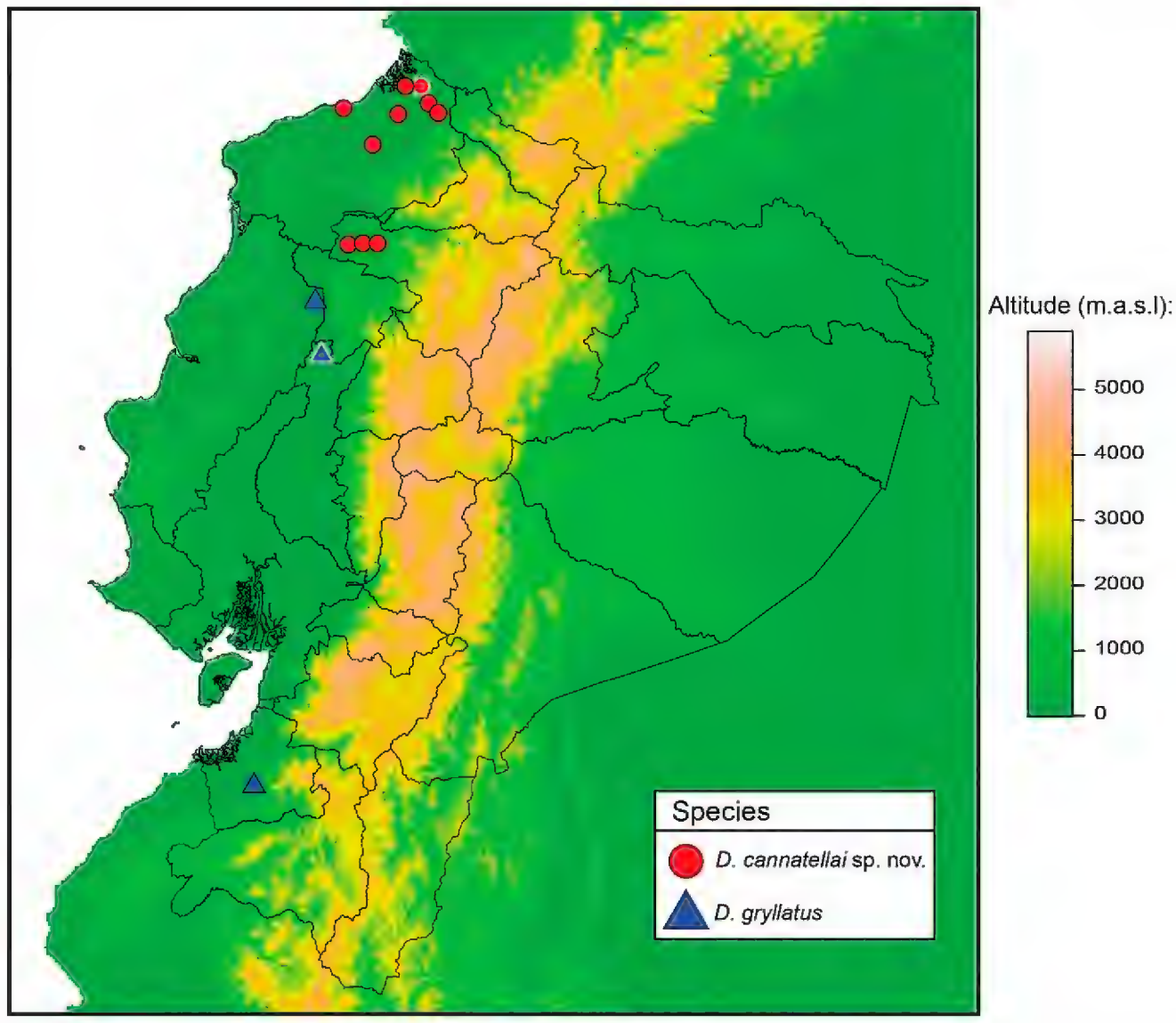

Figure 16. Distribution of the species *Dendropsophus cannatellai* sp. nov. and *D. gryllatus*. Localities are based of specimens deposited at Pontificia Universidad Católica del Ecuador, QCAZ Museum, Duellman (1974), and Michelsohn et al. (2022). Shapes with white outlines represent type localities. All known localities for both species are shown.

Our examination of *D. gryllatus* shows that glands on the pectoral region are present, a character state also reported by Orrico et al. (2021) for topotypic specimens deposited at the Museum of Zoology, University of São Paulo, Brazil. Presence of pectoral glands is congruent with its phylogenetic position because that character state has been proposed as a synapomorphy for the *D. leucophyllatus* species group (Orrico et al. 2021). The phylogenetic position of *D. gryllatus* is also congruent with its geographical distribution as its sister species, *D. cannatellai* sp. nov., is the only other species of the group present in the Chocó region.

Dendropsophus gryllatus and *D. cannatellai* sp. nov. are sister species with either allopatric or parapatric distribution ranges (Fig. 7). Future studies should explore the transition region between them because a contact zone could result in sporadic introgression or reproductive character displacement in advertisement calls. *Dendropsophus gryllatus* is an uncommon species, that is considered threatened with extinction. It has been assigned to the Endangered (UICN 2024) and Critically Endangered categories (Ortega-Andrade et al. 2021). Its high risk of extinction contrasts with most species of *Dendropsophus*, a genus where 91% of the species are assigned to the Least Concern category (93 species our of 102 evaluated; IUCN 2024). Only two *Dendropsophus* species are Critically Endangered and six are Endangered. Therefore, *D. gryllatus* is peculiar within a species group where most species are abundant in anthropic habitats. The main reason for its high extinction risk was the low number of known populations (two populations, according to IUCN 2024) or low extent of occurrence (1.4 km^2 according to Ortega-Andrade 2021). However, those evaluations are based on incomplete data or biased estimates of extent of occurrence (Fig. 16). A reevaluation of *D. gryllatus* extinction risk category is likely to result in a lower extinction risk category, more in agreement with the generalized low extinction risk of the genus *Dendropsophus*.

Variation in advertisement calls

A comparison with the study by Wells and Schwartz (1984b) reveals extensive variation in the acoustic parameters of *D. ebraccatus*. Their report on the primary note reveals a mean duration of 178 ms with a coefficient of variation (CV) of 12%, a pulse rate of 94 pulses per second (CV = 6%), a rise time of 131 ms (CV = 10%), and a proportional rise time of 0.73 (range: 0.54–0.92), which aligns with our measurements for *D. ebraccatus*. Ohmer et al. (2009), measured male advertisement calls from five genetically divergent regions in Costa Rica and Panama. In our study, the duration of the primary note was 0.21 ± 0.02 s, whereas Ohmer et al. (2009) found it to range from 0.14 s (Northeast CR) to 0.19 s (Southwest CR). The dominant frequency of the primary note in our study averaged 2502.86 ± 980.60 Hz, while Ohmer et al. reported frequencies between 2528.26 Hz (Northeast CR) and 2708.91 Hz (Southeast CR). Regarding the first secondary click, our data show a duration of 0.05 ± 0.01 s, while Ohmer et al. recorded click durations from 0.019 s

(Panama) to 0.039 s (Southeast CR). Additionally, our inter-note interval was 0.08 ± 0.01 s, compared to Ohmer et al.'s range of 0.020 s (Southwest CR) to 0.15 s (Northwest CR). Interpopulation call differences and evidence of genetic isolation among populations from Costa Rica and Panamá (Touchon et al. 2024) could indicate the existence of cryptic species.

The difference in dominant frequency between *D. gryllatus* and *D. cannatellai* could be a consequence of the smaller size of *D. gryllatus* as it is well known that size and spectral variables are inversely correlated (Köhler et al. 2017). Nevertheless, the non-overlapping values in dominant frequency and pulse rate between both species suggest the existence of prezygotic reproductive barriers between them, regardless of size differences.

In the analysis of acoustic variables for *D. cannatellai* and *D. gryllatus*, several traits fall into either static or dynamic categories based on Gerhardt's (1991) thresholds. The coefficient of variation (CV) was calculated as CV = SD*100/mean. For *D. cannatellai*, the dominant frequency of the call (CV = 4.76%) and the dominant frequency of the primary note (CV = 4.31%) are static traits, suggesting a role in species recognition or individual identity. Meanwhile, dynamic traits include the duration of the first secondary click (CV = 33.33%), number of pulses of the primary note (CV = 15.6%), and pulse repetition rate of the primary note (CV = 6.76%). For *D. gryllatus*, static traits include the dominant frequency of the call (CV = 2.59%) and the dominant frequency of the primary note (CV = 2.14%), while dynamic traits include the duration of the first secondary click (CV = 66.67%), the number of pulses of the primary note (CV = 32.13%), and the pulse repetition rate of the primary note (CV = 32.24%). Although the calls of both species share a similar structure, they differ in frequency and pulse rate, two variables that are among the most useful to detect species limits (Köhler et al. 2017).

Acknowledgments

Field and laboratory work in Ecuador were funded by Secretaría Nacional de Educación Superior, Ciencia, Tecnología e Innovación del Ecuador SENESCYT (Arca de Noé initiative; SRR and Omar Torres principal investigators) and grants from Pontificia Universidad Católica del Ecuador, Dirección General Académica and Dirección de Investigación. We thank the director of the DIRBE, Hugo Navarrete. Andrés Merino-Viteri, for his assistance with the script for creating the distribution map and for giving us access to the Balsa de los Sapos for the breeding of our individuals and tadpoles. We also thank Freddy Almeida for his help in setting up terrariums at Balsa and for taking care of tadpoles and frogs. We are also grateful to Julián Faivovich and Emilio Trujillo for their help reviewing the manuscript. Omar Torres, for his guidance in the use of software and in details of the systematic methodology. Santiago Burneo, for helping with the niche modeling. Gabriela B. Bittencourt and Jeffrey Streicher (Natural History Museum of London) for funding for fieldwork at Silanche. To Yerka Sagredo, Diego Paucar, and Mylena Masache for accompanying us on the field. We are thankful to the staff at the QCAZ Museum for their work in specimen preservation, especially Santiago Guamán, Fernando Ayala, and Diego Paucar. Jhael A. Ortega, for her guidance in reviewing and sexing specimens. For specimen collection, we thank Alex Achig, Diego Almeida, Verónica Andrade, Néstor Acosta, Fernando Ayala, Gabriela Bittencourt, M. Bustamente, David Cannatella, Felipe Campos, Luis Coloma, Stella de la Torre, Ricardo Gavilanez, Catherine Graham, Gabriela Granda, Fernanda Gordon, Santiago Guamán, Paulina Guarderas, Arturo Guasti, Rogerio Feijoo, Simón Lobos, Stephan Lötters, Andrea Manzano, Mylena Masache, Andrés Merino, Francy Mora, Kunam Nusirquia, Paulina Ordoñez, Lorena Orejuela, Diego Paucar, Morley Read, Myriam Rivera, Giovanna Rodríguez, Yerka Sagredo, Juan Carlos Santos, Jeffrey Streicher, Elicio Tapia, Ítalo Tapia, Diego Tirira, Justin Touchon, S. Valdiviezo, David Velalcázar, Mark Weiner, Alex Widmer, John Wiens. We thank Ulisses Caramaschi and one anonymous reviewer for their helpful comments to our manuscript.

References

Caminer MA, Mila B, Jansen M, Fouquet A, Venegas PJ, Chavez G, Lougheed SC, Ron SR (2017) Systematics of the *Dendropsophus leucophyllatus* species complex (Anura: Hylidae): Cryptic diversity and the description of two new species. PLoS ONE 12(3): e0171785. https://doi.org/10.1371/journal.pone.0171785

Chek A, Lougheed S, Bogart J, Boag P (2001) Perception and history: molecular phylogeny of a diverse group of neotropical frogs, the 30-chromosome *Hyla* (Anura: Hylidae). Molecular Phylogenetics and Evolution 18: 370–385. https://doi.org/10.1006/mpev.2000.0889

Chernomor O, Von Haeseler A, Minh BQ (2016) Terrace aware data structure for phylogenomic inference from supermatrices. Systematic Biology 65(6): 997–1008. https://doi.org/10.1093/sysbio/syw037

Cornell Lab of Ornithology (2003–2008) Raven Pro. Version 1.3. Bioacoustic Research Program. New York, USA.

Deng W, Maust BS, Nickle DC, Learn GH, Liu Y, Heath L, Kosakovsky Pond SL, Mullins JI (2010) DIVEIN: a web server to analyze phylogenies, sequence divergence, diversity, and informative sites. Biotechniques 48(5): 405–408. https://doi.org/10.2144/000113370

Duellman WE (1970) The hylid frogs of Middle America. Natural History Museum, University of Kansas. https://doi.org/10.5962/bhl.title.2835

Duellman WE (1973) Descriptions of new hylid frogs from Colombia and Ecuador. Herpetologica 29(3): 219–227.

Duellman WE (1974) A reassessment of the taxonomic status of some Neotropical hylid frogs. Occasional Papers of the Museum of Natural History, University of Kansas 27: 1–27.

Duellman WE, Lehr E (2009) Terrestrial breeding frogs (Strabomantidae) in Perú. Natur- und Tier-Verlag, Naturwissenschaft, Münster.

Faivovich J, Haddad CF, Garcia PC, Frost DR, Campbell JA, Wheeler WC (2005) Systematic review of the frog family Hylidae, with special reference to Hylinae: phylogenetic analysis and taxonomic revision. Bul-

letin of the American Museum of natural History 2005(294): 1–240. https://doi.org/10.1206/0003-0090(2005)294[0001:SROTFF]2.0.CO;2

Fick SE, Hijmans RJ (2017) WorldClim 2: new 1-km spatial resolution climate surfaces for global land areas. International Journal of Climatology 37(12): 4302–4315. https://doi.org/10.1002/joc.5086

Frost DR (2024) Amphibian Species of the World: An Online Reference. Version 6.2 (May 23, 2024). Electronic Database accessible at https://amphibiansoftheworld.amnh.org/index.php. American Museum of Natural History, New York, USA. https://doi.org/10.5531/db.vz.0001

Gerhardt HC (1991) Female mate choice in treefrogs: static and dynamic acoustic criteria. Animal Behaviour 42(4): 615–635. https://doi.org/10.1016/S0003-3472(05)80245-3

Gosner KL (1960) A simplified table for staging anuran embryos and larvae with notes on identification. Herpetologica 16(3): 183–190. https://www.jstor.org/stable/3890061

Hime PM, Lemmon AR, Moriarty Lemmon E, Prendini E, Brown JM, Thomson RC, Kratovil JD, Noonan BP, Pyron RA, Peloso PL (2021) Phylogenomics reveals ancient gene tree discordance in the Amphibian Tree of Life. Systematic Biology 70(1): 49–66. https://doi.org/10.1093/sysbio/syaa034

Hillis DM (2019) Species Delimitation in Herpetology. Journal of Herpetology 53: 3–12. https://doi.org/10.1670/18-123

Hoang DT, Chernomor O, Von Haeseler A, Minh BQ, Vinh LS (2018) UFBoot2: Improving the ultrafast bootstrap approximation. Molecular Biology and Evolution 35(2): 518–522. https://doi.org/10.1093/molbev/msx281

Hoorn C, Wesselingh FP, Ter Steege H, Bermudez MA, Mora A, Sevink J, Sanmartín I, Sanchez-Meseguer A, Anderson C, Figueiredo J (2010) Amazonia through time: Andean uplift, climate change, landscape evolution, and biodiversity. Science 330(6006): 927–931. https://doi.org/10.1126/science.1194585

IUCN (2024) The IUCN Red List of Threatened Species. Version 2024-1. https://www.iucnredlist.org [Accessed on August 20, 2024]

Katoh K, Misawa K, Kuma K, Miyata T (2002) MAFFT: a novel method for rapid multiple sequence alignment based on Fast Fourier Transform. Nucleic Acids Research 30(14): 3059–3066. https://doi.org/10.1093/nar/gkf436

Karger DN, Wilson AM, Mahony C, Zimmermann NE (2021) Global daily 1 km land surface precipitation based on cloud cover-informed downscaling. Scientific Data 2021(8): 1–18. https://doi.org/10.1038/s41597-021-01084-6

Kass JM, Pinilla-Buitrago GE, Paz A, Johnson BA, Grisales-Betancur V, Meenan SI, Attali D, Broennimann O, Galante PJ, Maitner BS, Owens HL, Varela S, Aiello-Lammens ME, Merow C, Blair ME, Anderson RP (2023) Wallace 2: a shiny app for modeling species niches and distributions redesigned to facilitate expansion via module contributions. Ecography 2023(3): e06547. https://doi.org/10.1111/ecog.06547

Kearse M, Moir R, Wilson A, Stones-Havas S, Cheung M, Sturrock S, Buxton S, Cooper A, Markowitz S, Duran C (2012) Geneious Basic: an integrated and extendable desktop software platform for the organization and analysis of sequence data. Bioinformatics 28(12): 1647–1649. https://doi.org/10.1093/bioinformatics/bts199

Köhler J, Jansen M, Rodriguez A, Kok PJ, Toledo LF, Emmrich M, Glaw F, Haddad CF, Roedel M-O, Vences M (2017) The use of bioacoustics in anuran taxonomy: theory, terminology, methods and recommendations for best practice. Zootaxa 4251(1): 1–124. https://doi.org/10.11646/zootaxa.4251.1.1

Maddison WP (2008) Mesquite: a modular system for evolutionary analysis. Evolution 62: 1103–1118. https://doi.org/10.1111/j.1558-5646.2008.00349.x

Michelsohn MJ, Barrow LN, Moretta M, Achig-Vega A, Nusirwuia K, Ron SR (2022) Geographic distribution notes. *Dendropsophus gryllatus* (Pacific Lowland Treefrog). Herpetological Review 53(2): 257–258.

Ministerio del Ambiente del Ecuador (2013) Sistema de Clasificación de los Ecosistemas del Ecuador Continental. Subsecretaría de Patrimonio Natural, Quito, Ecuador.

Nguyen LT, Schmidt HA, Von Haeseler A, Minh BQ (2015) IQ-TREE: A fast and effective stochastic algorithm for estimating maximum likelihood phylogenies. Molecular Biology and Evolution 32(1): 268–274. https://doi.org/10.1093/molbev/msu300

Ohmer ME, Robertson JM, Zamudio KR (2009) Discordance in body size, colour pattern, and advertisement call across genetically distinct populations in a Neotropical anuran (*Dendropsophus ebraccatus*). Biological Journal of the Linnean Society 97: 298–313. https://doi.org/10.1111/j.1095-8312.2009.01210.x

Orrico VG, Grant T, Faivovich J, Rivera-Correa M, Rada MA, Lyra ML, Cassini CS, Valdujo PH, Schargel WE, Machado DJ (2021) The phylogeny of Dendropsophini (Anura: Hylidae: Hylinae). Cladistics 37(1): 73–105. https://doi.org/10.1111/cla.12429

Ortega-Andrade HM, Meza-Ramos P, Cisneros-Heredia DF, Yánez-Munoz MH, Altamirano-Benavidez M (2010) Los anfibios y reptiles del Chocó Esmeraldeño. In: Serie herpetofauna del Ecuador: el Chocó Esmeraldeño. Monografía. Museo Ecuatoriano de Ciencias Naturales, Quito, Ecuador, 95–232.

Ortega-Andrade HM, Rodes Blanco M, Cisneros-Heredia DF, Guerra Arévalo N, López de Vargas-Machuca KG, Sánchez-Nivicela JC, Armijos-Ojeda D, Cáceres Andrade JF, Reyes-Puig C, Quezada Riera AB (2021) Red List assessment of amphibian species of Ecuador: A multidimensional approach for their conservation. PloS ONE 16(5): e0251027. https://doi.org/10.1371/journal.pone.0251027

Phillips SJ, Dudík M (2008) Modeling of species distributions with Maxent: new extensions and a comprehensive evaluation. Ecography 31(2): 161–175. https://doi.org/10.1111/j.0906-7590.2008.5203.x

Pintanel P, Tejedo M, Merino-Viteri A, Almeida-Reinoso F, Salinas-Ivanenko S, López-Rosero AC, Llorente GA, Gutiérrez-Pesquera LM (2022) Elevational and local climate variability predicts thermal breadth of mountain tropical tadpoles. Ecography 2022: e05906. https://doi.org/10.1111/ecog.05906

Pirani RM, Peloso PL, Prado JR, Polo ÉM, Knowles LL, Ron SR, Rodrigues MT, Sturaro MJ, Werneck FP (2020) Diversification history of clown tree frogs in Neotropical rainforests (Anura, Hylidae, *Dendropsophus leucophyllatus* group). Molecular Phylogenetics and Evolution 150: 106877. https://doi.org/10.1016/j.ympev.2020.106877

Pontificia Universidad Católica del Ecuador (2021) Base de datos de la colección de anfibios del Museo de Zoología QCAZ. Versión 2021.0. bioweb.bio/portal [February 6, 2021]

QGIS.org (2023) QGIS Geographic Information Systems.

R Core Team (2023) R: A Language and Environment for Statistical Computing. R Foundation for Statistical Computing, Vienna, Austria. https://www.R-project.org/

Rivera-Correa M, Orrico VG (2013) Description and phylogenetic relationships of a new species of treefrog of the *Dendropsophus leucophyllatus* group (Anura: Hylidae) from the Amazon basin of Colombia and with an exceptional color pattern. Zootaxa 3686(4): 447–460. https://doi.org/10.11646/zootaxa.3686.4.3

Robertson JM, Duryea MC, Zamudio KR (2009) Discordant patterns of evolutionary differentiation in two Neotropical treefrogs. Molecular Ecology 18: 1375–1395. https://doi.org/10.1111/j.1365-294X.2009.04126.x

Ron SR, Guayasamin JM, Menéndez-Guerrero PA (2011) Biodiversity and Conservation Status of Ecuadorian Amphibians. In: Heatwole H, Barrio-Amoros C, Wilkinson HW (Eds) Amphibian Biology, Vol. 9, Part 2. Surrey Beatty & Sons Pty. Ltd., Australia, 129–170.

Ron SR, Merino-Viteri A, Ortiz DA (2024) Anfibios del Ecuador. Version 2024.0. https://bioweb.bio/faunaweb/amphibiaweb/

Savage JM (2002) The amphibians and reptiles of Costa Rica: a herpetofauna between two continents, between two seas. The University of Chicago Press, Chicago.

Simpson N, Reyes-Puig C, Tobar C, Yánez-Muñoz M (2013) Herpetofauna en áreas prioritarias para la conservación: el sistema de Reservas Jocotoco y Ecominga. MECN-Jocotoco-ECOMINGA 2013.

Swets JA (1988) Measuring the accuracy of diagnostic systems. Science 240(4857): 1285–1293. https://doi.org/10.1126/science.3287615

To TH, Jung M, Lycett S, Gascuel O (2016) Fast dating using least-squares criteria and algorithms. Systematic Biology 65(1): 82–97. https://doi.org/10.1093/sysbio/syv068

Touchon JC, McMillan WO, Ibáñez R, Lessios HA (2024) Flexible oviposition behavior enabled the evolution of terrestrial reproduction. Proceedings of the National Academy of Sciences 121: e2312371121. https://doi.org/10.1073/pnas.2312371121

Vences M (2020) The promise of next-generation taxonomy. Megataxa 1(1): 35–38. https://doi.org/10.11646/megataxa.1.1.6

Wells KD, Schwartz JJ (1984a) Vocal communication in a neotropical treefrog, *Hyla ebraccata*: advertisement calls. Animal Behaviour 32(2): 405–420. https://doi.org/10.1016/S0003-3472(84)80277-8

Wells KD, Schwartz JJ (1984b) Vocal communication in a neotropical treefrog, *Hyla ebraccata*: aggressive calls. Behaviour 91(1–3): 128–145. https://doi.org/10.1163/156853984X00254

Wickham H, Chang W (2016) Package 'ggplot2.' Create elegant data visualizations using the grammar of graphics. Version 2: 1–189.

Wiley EO (1978) The evolutionary species concept reconsidered. Systematic Zoology 27: 17–26. https://doi.org/10.2307/2412809

Supplementary material 1

Table S1. Information of examined specimens

Authors: P. Doménica Aguirre
Data type: xlsx
Copyright notice: This dataset is made available under the Open Database License (http://opendatacommons.org/licenses/odbl/1.0). The Open Database License (ODbL) is a license agreement intended to allow users to freely share, modify, and use this Dataset while maintaining this same freedom for others, provided that the original source and author(s) are credited.
Link: https://doi.org/10.3897/evolsyst.9.135431.suppl1

Supplementary material 2

Figure S1. Complete maximum likelihood tree of *Dendropsophus*

Authors: P. Doménica Aguirre, Santiago R. Ron
Data type: pdf
Explanation note: Numbers at branches show SH-aLRT values (before slash) and ultrafast bootstrap support values (after slash).
Copyright notice: This dataset is made available under the Open Database License (http://opendatacommons.org/licenses/odbl/1.0). The Open Database License (ODbL) is a license agreement intended to allow users to freely share, modify, and use this Dataset while maintaining this same freedom for others, provided that the original source and author(s) are credited.
Link: https://doi.org/10.3897/evolsyst.9.135431.suppl2

Supplementary material 3

Figure S2. Complete chronogram of *Dendropsophus* based on the best ML tree

Authors: P. Doménica Aguirre, Santiago R. Ron
Data type: pdf
Explanation note: Numbers in the nodes represent divergence times in Mya; blue numbers represent support values.
Copyright notice: This dataset is made available under the Open Database License (http://opendatacommons.org/licenses/odbl/1.0). The Open Database License (ODbL) is a license agreement intended to allow users to freely share, modify, and use this Dataset while maintaining this same freedom for others, provided that the original source and author(s) are credited.
Link: https://doi.org/10.3897/evolsyst.9.135431.suppl3

Supplementary material 4

Figure S3. Principal component analysis of the vocalizations of *D. ebraccatus*, *D. cannatellai* sp. nov. and *D. gryllatus*

Authors: P. Doménica Aguirre
Data type: pdf
Copyright notice: This dataset is made available under the Open Database License (http://opendatacommons.org/licenses/odbl/1.0). The Open Database License (ODbL) is a license agreement intended to allow users to freely share, modify, and use this Dataset while maintaining this same freedom for others, provided that the original source and author(s) are credited.
Link: https://doi.org/10.3897/evolsyst.9.135431.suppl4

Supplementary material 5

Figure S4. Phylogenetic network for the nuclear gene tyrosinase between *D. cannatellai* sp. nov. and *D. gryllatus*

Authors: Santiago R. Ron
Data type: jpg
Copyright notice: This dataset is made available under the Open Database License (http://opendatacommons.org/licenses/odbl/1.0). The Open Database License (ODbL) is a license agreement intended to allow users to freely share, modify, and use this Dataset while maintaining this same freedom for others, provided that the original source and author(s) are credited.
Link: https://doi.org/10.3897/evolsyst.9.135431.suppl5

Supplementary material 6

Table S2. Bioclimatic variables used in environmental niche models and environmental envelope analyses

Authors: P. Doménica Aguirre
Data type: docx
Copyright notice: This dataset is made available under the Open Database License (http://opendatacommons.org/licenses/odbl/1.0). The Open Database License (ODbL) is a license agreement intended to allow users to freely share, modify, and use this Dataset while maintaining this same freedom for others, provided that the original source and author(s) are credited.
Link: https://doi.org/10.3897/evolsyst.9.135431.suppl6

Supplementary material 7

Table S3. Summary statistics for ecological niche models obtained from Wallace 2 package

Authors: P. Doménica Aguirre
Data type: xlsx
Copyright notice: This dataset is made available under the Open Database License (http://opendatacommons.org/licenses/odbl/1.0). The Open Database License (ODbL) is a license agreement intended to allow users to freely share, modify, and use this Dataset while maintaining this same freedom for others, provided that the original source and author(s) are credited.
Link: https://doi.org/10.3897/evolsyst.9.135431.suppl7

Supplementary material 8

Table S4. Uncorrected p-genetic distances for the gen 16S between populations of *D. ebraccatus*, *D. cannatellai* sp. nov. and *D. gryllatus*

Authors: P. Doménica Aguirre
Data type: xlsx
Copyright notice: This dataset is made available under the Open Database License (http://opendatacommons.org/licenses/odbl/1.0). The Open Database License (ODbL) is a license agreement intended to allow users to freely share, modify, and use this Dataset while maintaining this same freedom for others, provided that the original source and author(s) are credited.
Link: https://doi.org/10.3897/evolsyst.9.135431.suppl8